Journal of Geography and Geology; Vol. 15, No. 1; 2023
ISSN 1916-9779 E-ISSN 1916-9787
Published by Canadian Center of Science and Education

# Cascadia Earthquake-Triggered Rockslide Burial of Beeswax Galleon Wreck Timbers in a Sea Cliff Wave-Cut Platform Site, North Smuggler Cove, Oregon, USA

Curt D. Peterson[1], Scott Williams[2] & Craig Andes[3]

[1] Geology Department, Portland State University, Portland, Oregon, United States

[2] Maritime Archaeological Society, Astoria, Oregon, United States

[3] Garibaldi, Oregon, United States

Correspondence: Curt Peterson, Geology Department, Portland State University, Portland, OR., 97207, United States. Tel: 1-503-730-9266. E-mail: curt.d.peterson@gmail.com

Received:January 27, 2023 Accepted: March 2, 2023 Online Published: March 6, 2023

doi: 10.5539/jgg.v15n1p1 URL: https://doi.org/10.5539/jgg.v15n1p1

**Abstract**

Shipwreck timbers (n=27) from the Spanish galleon Santo Cristo de Burgos, also known as the Beeswax Wreck (lost in 1693), are examined for origins of multiple, simultaneous rockslide burials that protected and preserved the timbers on an intertidal wave-cut platform in the small Smuggler Cove in the Northern Oregon coast. The rockslides (n=3–4) that buried the shipwreck timbers are compared to nearby historic rockslide analogs to better establish the mechanisms of boulder distributions on the wave-cut platform. Large boulders (n=20), generally ≥1.0 m intermediate diameter, in the North Smuggler Cove (NSC) timber burial site were measured for estimated mass (1–41 t) and alongshore distribution below small gullies that routed the boulders to the wave-cut platform from overlying short (~100 m distance) but steep hillslopes (40–60% gradient). The multiple independent rockslides in the NSC site, dated to ~300 years by the buried Beeswax Wreck timbers, showed catastrophic, simultaneous activation by a widespread trigger. Anomalous rainfall and/or storm wave attack are unlikely mechanisms for these rockslide activations due to 1) hillslope protections from extended-upslope surface water discharge and 2) sea cliff protection from direct storm wave impacts. The most likely widespread trigger for rockslide activation in the NSC site is seismic ground shaking from an earthquake in the Central Cascadia subduction zone. Modern storm wind velocities (>10 $s^{-1}$ sustained velocity and 170–225° bearing) and storm surge generated rip currents (≥0.5 km offshore distance) indicate that Beeswax Wreck timbers could have been transported north (1–10 km) to Smuggler Cove, within several winter seasons after the breakup of the Santo Cristo de Burgos. The most likely seismic trigger that could have activated the multiple rockslides in the NSC site, shortly after the brief accumulation of shipwreck timbers on the narrow, intertidal wave-cut platform in Smuggler Cove, is the 1700 Cascadia great earthquake ($M_w$~9.0). Additional sea cliff rockslide sites (n=8) in the central Cascadia margin are suggested for further investigations of seismically activated slope failures by the 1700 Cascadia great earthquake.

**Keywords:** galleon, Beeswax Wreck, timber artifacts, driftwood transport, rockslide burial, Cascadia earthquake

## 1. Introduction

In this article, large boulders that bury shipwreck timbers from a Spanish galleon Santo Cristo de Burgos, lost in 1693 (Williams et al., 2017), are used to establish the age and origin of rockslides from sea cliffs and overlying hillslopes on the north side of a small cove in the central Cascadia subduction zone (Figure 1). Debris from the shipwreck included beeswax blocks, porcelain sherds, and tropical wood, which were distributed across the Nehalem Bay spit and tidal flats, located about 10 km south of the small cove (Mashall, 1984; Williams et al., 2018). The distributions of Beeswax Wreck artifacts across the bay spit were eventually attributed to nearfield tsunami inundations resulting from the great Cascadia earthquake ($M_w$~9.0) that ruptured through the Cascadia subduction zone in 1700 (Darienzo et al., 1994; Atwater et al., 1995; Satake et al., 1996). In this article, the likely conditions of Beeswax Wreck timber transport around a large headland and accumulation within the small cove are estimated from modern transport conditions that are associated with major winter storms. Such conditions would have had to occur between the wreck of the Santo Cristo de Burgos and the rockslide burial of shipwreck timbers. Multiple simultaneous rockslides in gullies from adjacent hillslopes on the north side of the small cove are

attributed to a seismic trigger rather than extreme storm conditions, as the cove setting would have been the protected against severe storm conditions (Peterson et al., 2022). In this article, the great Cascadia earthquake, dated by its transpacific tsunami of January 26, 1700 (Satake et al., 1996), is proposed to have been the seismic trigger for the rockslides, that buried the Beeswax Wreck timbers. Additional sea cliff sites that 1) could have trapped dateable driftwood and 2) show evidence of rockslide debris on bedrock platforms are presented for the further testing of seismically triggered slope failures along the coastline of the Central Cascadia Margin.

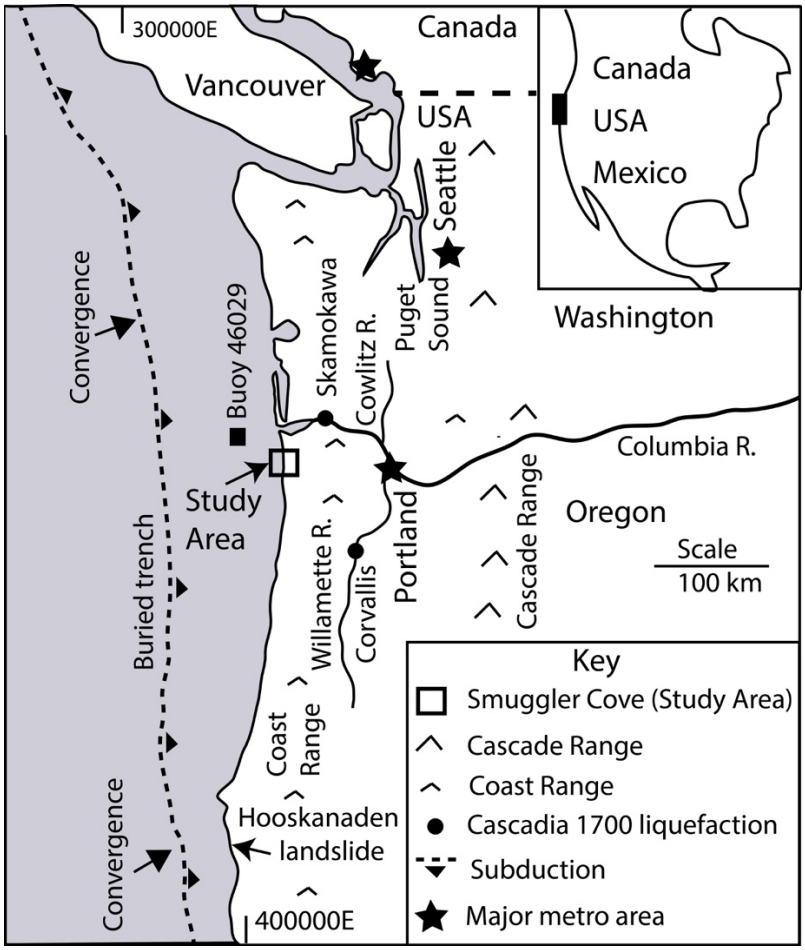


Figure 1. Map of Central Cascadia Margin study region and location of the Smuggler Cove study area

Mapped study region features include1) the buried trench (dashed line with down-dip triangles) in Central Cascadia Margin subduction zone, as spanned by the 1700 $M_w$~9.0 rupture, 2) Cascade Range volcanoes (large pyramids), 3) uplifted Coastal Ranges (small pyramids), 4) NOAA buoy 46029 (solid square), 5) large scale paleoliquefaction sites (solid circles), 6) major metro areas (Portland, Seattle, Vancouver). A sea cliff landslide (Hooskanaden) is thought to have been activated or reactivated by the Cascadia great earthquake ($M_w$~9.0) in 1700 (Alberti et al., 2020; Kingen, 2021). The location of the Smuggler Cove study area is shown (boxed), due west of Portland, Oregon.

## 2. Background

### *2.1 Beeswax Galleon Shipwreck*

Between 2006 and 2010 a team of archaeologists, geologists, and collectors was formed to unravel the mystery of beeswax blocks, Asian porcelain sherds, and tropical wood artifacts that were strewn across the sand spit of Nehalem Bay, Oregon (Figure 2) (Giesecke, 2007; Williams, 2007). The artifacts were tentatively traced to a lost Spanish galleon, possibly the San Francisco Xavier lost in 1705 (Giesecke, 2007) but the mechanism for the distribution of artifacts across the bay spit could not be explained. After geological studies established that tsunami cobbles and boulders were draped across the surface of the sand spit the across spit distribution of artifacts were attributed to nearfield tsunami surges (Peterson et al., 2011) resulting from the last Cascadia megathrust rupture ($M_w$~9.0) in 1700 (Satake et al., 1996). A renewed search of Spanish documents showed that another galleon Santo

Cristo de Burgos had been lost in 1693, thereby permitting overland transport of artifacts by the 1700 Cascadia tsunami surges (Williams et al., 2017). The coincidence of the Spanish galleon shipwreck, referred to informally as the Beeswax Wreck, followed by the 1700 Cascadia earthquake and associated tsunami, explained the mystery of Beeswax Wreck artifacts transported across the bay spit and adjacent tidal flats (Williams et al., 2018). Historically the Beeswax Wreck was described as located along the Nehalem Bay spit. Wreckage included sections of the lower hull, mast, mast step, ribs, and other wood debris, along with a section of deck or one of the deck castles at the river mouth on the south end of the sand spit adjacent to the tidal inlet of the Nehalem River. The amount of tropical wood, historically reported as 'teak', on the bay spit and Manzanita beaches was not well constrained, but it reportedly still exceeded many wagonloads, as late as the early-1900s (Paul See, pers. comm., 2008). Beach and foredune progradation have completely buried the early-historic strandlines of beaches and the seaward deposits of the Nehalem Bay sand spit from which the Beeswax Wreck timbers were recovered by the early European settlers. Some wreck debris was also described to be lodged against the base of Neahkahnie Mountain headland, where "no man dare go" (Astoria Daily Budget, 1894). Most recently, porcelain sherds and some square cut and notched shipwreck timbers have been found in a small embayment, Smuggler Cove, located about 7–12 km north of the Nehalem Bay spit, as shown in Figure 2. It was suspected that the artifacts were from the Beeswax Wreck, but it was unknown how the artifacts could have reached the small cove, located north of the large Neahkahnie Mountain headland. What was known was that the shipwreck timbers had been entrapped by large boulders lying on a wave-cut bedrock platform and in adjacent sea caves in the north side of Smuggler Cove, referred to here as the North Smuggler Cove (NSC) site. In this study, the mechanisms of potential timber transport and preservation of shipwreck timbers in the NSC site are investigated, as are possible origin(s) of the burial of shipwreck timbers by large boulders.

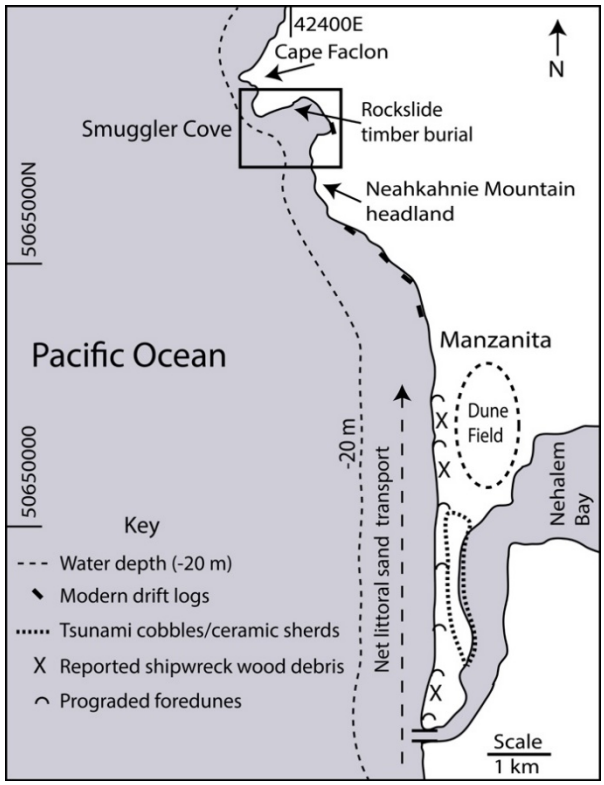


Figure 2. Map of Smuggler Cove and Nehalem Bay study area

Part A, Mapped study area features include 1) Smuggler Cove with Beeswax Wreck timber burial site (boxed), 2) Nehalem Bay sand spit with distribution of 1700 Cascadia nearfield tsunami cobbles and Beeswax porcelain and earthenware sherds (dotted line) (Peterson et a., 2011; Williams et al., 2017), 3) Holocene dune field north of Manzanita, Oregon (dashed circle), 4) northward direction of net littoral sand transport (dashed line with arrow) (Peterson et al., 2009), 5) estimated decadal depth of closure (-20 m dashed line) for littoral sand transport, and 6) modern drift logs from satellite images 2005-2022 (bold lines) (Goggle Earth Pro, 2022). Historically reported shipwreck timber sites (marked X) (Williams et al., 2018) are now buried by prograded foredunes (half circles).

*2.2 Strength of Earthquake Shaking in the Central Cascadia Subduction Zone*

The Cascadia subduction zone was only recently identified as being seismogenic (Peterson and Scheidegger, 1983). Due to a lack of major megathrust ruptures since European settlement, some uncertainties exist with regards to expected seismic ground accelerations that could arise from a future megathrust rupture. Large-scale paleoliquefaction features, including clastic dikes and sills (20–30 cm width) from the last Cascadia earthquake in 1700, have been reported at Skamokawa, Washington in the lower Columbia River valley (Peterson and Madin, 1997) and at Corvallis, Oregon, in the Willamette River valley, located respectively 70 and 150 km from the study site (Figure 1) (Peterson et al., 2014). Unexpectedly, such large-scale paleoliquefaction features (≥10 cm dike/sill widths) have yet to be identified in coastal deposits from the enigmatic 1700 Cascadia megathrust rupture. For these reasons it is important to independently gauge the strength of past great earthquake shaking from other geologic evidence along the coast of the Central Cascadia Margin. In this article, several unique rockslide factors in the Smuggler Cove study area are shown to require a widespread trigger for the rockslide activations (Figure 2). A seismic trigger is the most likely mechanism for the initiation of simultaneous independent rockslides in the NSC site. Previously, only one landslide activation or reactivation in the Central Cascadia Margin had been possibly attributed to the 1700 Cascadia megathrust rupture. It is the large Hooskanaden landslide complex in a southern Oregon sea cliff setting (Alberti et al., 2020; Kingen, 2021). Other sea cliff sites in the Central Cascadia Margin that could be searched for preserved records of rockslides initiated by the 1700 Cascadia great earthquake are presented at the end of this article.

*2.3 Smuggler Cove Geology*

The geologic development of Smuggler Cove and the encompassing rocky shorelines are important to understanding 1) accumulation of Beeswax Wreck timbers in Smuggler Cove and 2) the origins of rockslide boulders that buried the accumulated Beeswax Wreck timbers in the north side of Smuggler Cove. The Smuggler Cove embayment occurs in the Smuggler Cove and Astoria Formations, containing tuffaceous marine sandstones and mudstones, formed during the Oligocene-Miocene (Figure 3) (Cressy, 1974; Niem and Niem, 1985; Ma et al., 2009). The Smuggler Cove and Astoria formations in Smuggler Cove are bounded by sea cliff headlands of the Grand Ronde Basalt in the Columbia River Basalt Group (CRB). The erosion resistant CRB basalts make up most of the major coastal headlands in northern Oregon. The sandstones and mudstones in the Smuggler and Astoria Formations were less resistant to wave attack than the CRB basalts, thereby yielding to localized embayment. The unusual development of a small wave-protected cove in the center of the large headland massif makes for a unique catchment of littoral sand that is transported northward around the headland (Peterson et al., 2020). This unusual Smuggler Cove embayment will also prove to be important in the brief accumulation of Beeswax Wreck timbers, as discussed later in this study.

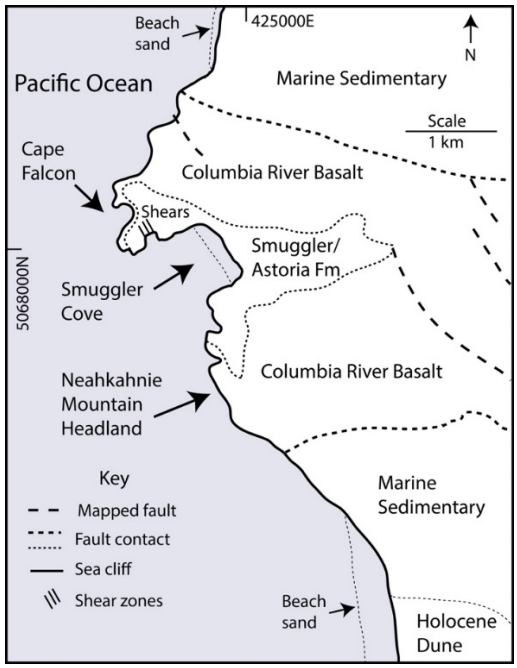


Figure 3. Generalized geology map of the Smuggler Cove study area

Mapped study area features include 1) Smuggler Cove and Astoria Formations of tuffaceous, basalt-sill-baked sandstones and mudstones, 2) Columbia River Basalt headlands, 3) Marine sedimentary rocks (undifferentiated in this map), 4) mapped fault offsets (bold dashed lines), 5) assumed fault contacts (dashed lines), and 5) Holocene dune field cover on the south flank of Neahkahnie Mountain. Several close-spaced shear zones (parallel lines) occur above sea caves in a shoreline indentation site that contains the boulder buried Beeswax Wreck timbers, as located on the north side of Smuggler Cove. Geology data are summarized from Cressy (1974), Niem and Niem (1985), and DOGAMI (2022a).

The Smuggler Cove Formation strata are either fault bounded against or invasively intruded by the CRB basalt units (Figure 3) (Niem and Niem, 1985). The Smuggler Cove strata show localized folding and small shear-fracture zones resulting from inelastic tectonic strain (K.M. Cruikshank, unpublished data, 2010). The sandstone and mudstone strata that are exposed along the north side of Smuggler Cove generally strike west–east and dip moderately (~25°) to the south (Cressy, 1974). The orientation of intact sandstone strata along the central north side of Smuggler Cove will have an important bearing on identifying rockslide boulders that buried Beeswax Wreck timbers in the north side of Smuggler Cove. The steep sea cliffs of indurated and/or basalt-sill-baked sandstone strata along the north side of Smuggler Cove are locally offset by small shear zones. Three sea caves and an indented or recessed shoreline have been eroded into sea cliffs that host several close spaced shear zones in the north side of Smuggler Cove (Figures 3 and 4). The shear zone related indentation of the sea cliffs in the north side of Smuggler Cove will be shown to have important impacts on local accumulations of Beeswax Wreck timbers, just prior to rockslide burial.

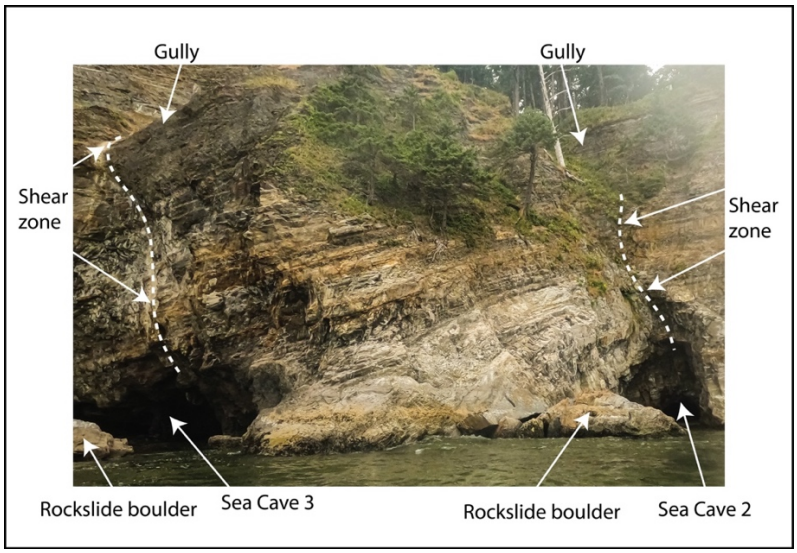


Figure 4. Photograph of sea caves and sea cliffs at the Beeswax Wreck timber burial site in Smuggler Cove

Near mid-tide levels show flooding of the entrances to two sea caves that are associated with small shear zones or joint sets in an area of shoreline indentation in the north side of Smuggler Cove (Figure 3). Rockslide boulders in front of the sea cave entrances are discriminated from intact bedrock strata by steeply inclined (near vertical) sedimentary strata (see Section 3.0 below). The large rockslide boulder in front of Sea Cave 2 pins three Beeswax Wreck timbers against the underlying bedrock wave-cut platform (see Section 4.1 below).

## 3. Methods

Square cut and notched shipwreck timbers were found in 2019, by one of these authors (Andes) in a recessed intertidal wave-cut platform and in adjacent sea caves, referred to here as the North Smuggler Cove (NCS) site (Figure 2). The timbers from the wave-cut platform were further observed by these authors during low tidal levels in 2020 to be entrapped against the underlying bedrock surface by overlying large boulders. The buried or pinned timbers that were partially exposed were mapped on high resolution drone images, using the distinctive overlying boulders as reference points. The boulder and underlying timber locations were entered into Google Earth satellite image KML files (Google Earth Pro, 2022) for georeferencing. Several of the shipwreck timbers were found wedged into fissures in the sea caves (Figure 5). Their positions in the seas caves (underground) were mapped by distances from the sea cave entrances. No surveys were conducted in the offshore subtidal water depths for shipwreck timbers, though distinctive boulders could be viewed by drone imaging through the shallowest water

columns. Several of the shipwreck timbers from the intertidal wave-cut platform were sampled by these authors and others in 2020, 2021, and 2022, for wood species identification and AMS radiocarbon dating. Selected shipwreck timbers that were recovered from the NSC site were analyzed for color (Munsell colors) shape, and asymmetry of surface degradation by marine boring organisms.

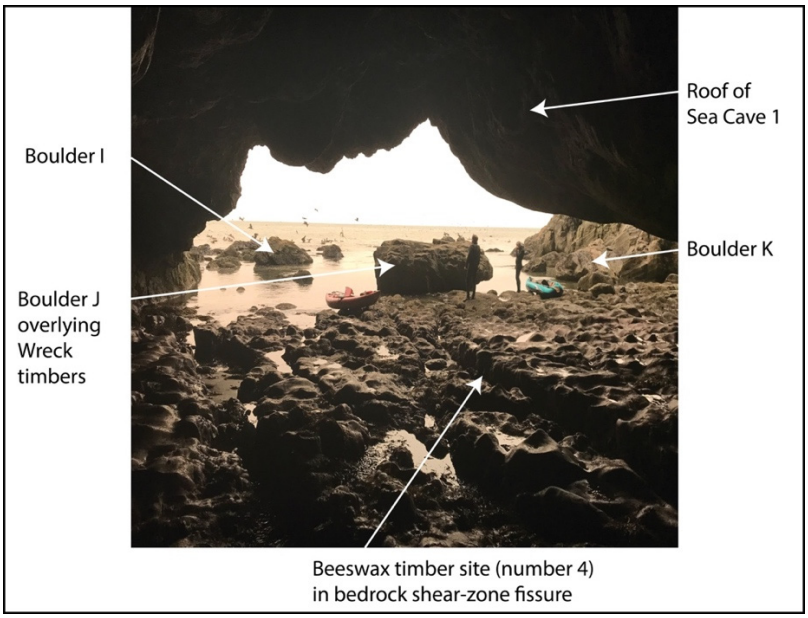


Figure 5. Photo of Sea Cave 1 with rockslide boulders in front of the sea cave entrance

Rockslide boulder J (2.0 m in length in shown long axis) buries two Beeswax Wreck timbers in front of Sea Cave 1 in the NSC site (see Section 4.1 below). Rockslide boulders I and K are shown in position relative to low tide level on the intertidal wave-cut bedrock platform that is developed in front of the Sea Cave 1 entrance. A large Beeswax Wreck timber beam (# 4 in Figure 6, below) was recovered from Sea Cave 1 where it was wedged into a shear zone fissure in the floor of the sea cave.

Representative large boulders (generally ≥1.0 m intermediate diameter), including some boulders that buried partially exposed Beeswax Wreck timbers, were identified for distribution, shape, orientation, unconfined shear strength, and size analyses (Peterson et al., 2022). Representative boulders were measured during on-the-ground surveys (2022) for strike and dip of sedimentary bedding, and angularity of shear plane edges on exposed boulder tops. The strata orientation data were used to discriminate rockslide boulders from possible bedrock protrusions. The strike and dip of rockslide boulders differed from the intact bedrock strata in adjacent sea cliffs. The angularity of shear plane edges on the large rockslide boulders (≥1.0 m intermediate diameter) were used to test whether rolling or tumbling of the large boulders occurred after initial rockslide emplacement on the wave-cut platform. The shear strengths of the boulder surfaces and shallow subsurface boulder materials, as exposed by rock hammer chipping, were measured by calibrated penetrometer. The locations of the distinctive boulders were transferred from drone images to Google Earth image KML files for georeferencing (Google Earth Pro, 2022). Apparent intermediate diameters of the large rockslide boulders were measured, to the nearest 0.25 m resolution, from the low-elevation drone images. The drone image measurements of boulder size were scaled or calibrated using on-the-ground measured dimensions of one centrally located boulder (boulder J, horizontal long axis 2.0 m and horizontal intermediate diameter 1.5 m) in the NSC site (Figure 5).

Rockslide boulder distributions on the wave-cut bedrock platform in the north side of Smuggler Cove were used to target potential rockslide sources by following adjacent gullies, which formed in the sea cliff tops (Figure 4) and extend upslope, to rockslide bodies and head scarps near a ridge top at about 100 m elevation. Gully widths, vertical relief, and slope gradients were measured with Nikon Forestry Pro ™ laser rangefinder/inclinometer. Rockslide debris that were exposed in scarps and rills were examined for soil development profiles, including soil A (organic) and B (accumulation) horizons (Birkeland, 1999), clast textural compositions, and unconfined shear strengths using calibrated penetrometer. The textural size classes that were estimated by scaled photographs for relative abundances include 1) fines (sand/fine gravel matrix), 2) angular pebbles (0.5–5 cm diameter), 3) angular cobbles 6–25 cm diameter) and 4) small angular boulders (>25 cm diameter). No large boulders were observed in the shallow surficial deposits, as exposed in small scarp offsets. Rockslide features and measurement sites were

georeferenced with a 12 channel GPS in WAS mode (±2 m optimal resolution, but ±5 m estimated potential error under forest cover).

## 4. Results

### *4.1 Mapped Abundances, Distributions, and Ages of Beeswax Wreck Timbers*

Square cut, square notched, and/or rounded shipwreck timbers (n=27) were buried by rockslide boulders on the intertidal wave-cut bedrock platform and/or pinned in small sea caves in the North Smuggler Cove (NSC) site, located on the north side of Smuggler Cove (Figures 2 and 6; Table 1). Several representative shipwreck timbers were sampled for radiocarbon AMS dating (Table 2). The field identification of shipwreck timber (wood) from the Philippines was aided by anomalous high density and color, such as Vitex parviflora (2.5Y 7/6 yellow) that is distinguished from local native conifer and hardwood driftwood. Calibrated ages of the shipwreck timbers (n=7 AMS dates), ranging cal 1425–1796 2σ, confirm that the origins of the shipwreck timbers were from the wreck of the Santo Cristo de Burgos or Beeswax Wreck (Williams et al., 2017, Williams et al., 2018). Twenty-three Beeswax Wreck timbers that were buried by rockslide boulders were identified in the subaerial wave-cut platform. Three Beeswax Wreck timbers (# 4, # 19 and # 20) were found wedged or pinned into fissures in the floors of Sea Caves 1 and 3 (Figure 6). One dense water-logged Beeswax Wreck timber (#15) was found pinned between boulders on the wave-cut platform. The dense, waterlogged Beeswax Wreck timbers are sufficiently negatively buoyant to resist resuspension by moderate wave surge. However, loosened Beeswax Wreck timbers are presumably susceptible to remobilization by the highest-wave-energy conditions in the NSC site. About 200–300 kilograms of Beeswax Wreck timber artifacts were recovered from the NSC site, as archived in the Columbia River Maritime Museum, Astoria, Oregon. The weights of the recovered Beeswax Wreck timbers, or timber fragments, range 5–100 kg. Most of the recovered Beeswax Wreck timbers, such as # 2, # 7 and # 11, show rounding of exterior surfaces, indicating significant abrasion during transport, prior to burial (Figure 7A). Some of the recovered Beeswax Wreck timbers, such as # 7 and # 11, demonstrate strong asymmetry of wood surface degradation (Figures 7B and 7C), with one side showing biogenic degradation by boring, pitting, and flaking, and the opposite side showing little to no degradation, where burial had largely protected the wood from exposure to oxygenated seawater and biogenic decomposition.

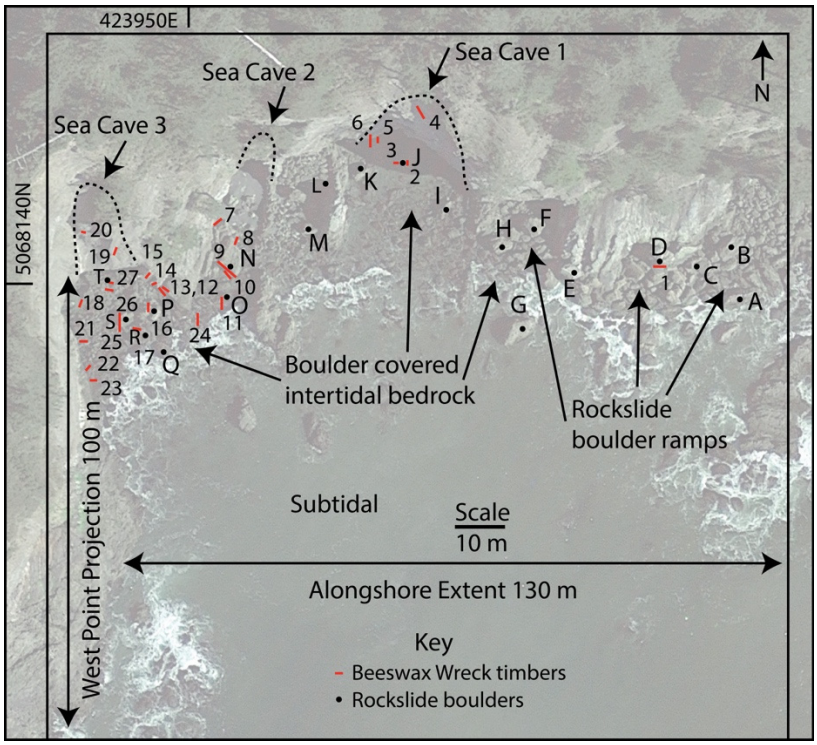


Figure 6. Map of Beeswax Wreck timbers and selected large rockslide boulders in the NSC site

Mapped features include 1) length scales of NSC site (double arrow lines), 2) Sea Caves (numbered 1–3), 3) mapped Beeswax Wreck timbers, n=27 (numbered red lines), 4) representative large boulders, n=20 (lettered solid circles) used for boulder size analyses. All the Beeswax Wreck timbers were buried under rockslide boulders, except timber numbers 4, 15, 19, and 20, which were wedged or pinned in fissures or between boulders. Mean tide

level at the time of this satellite image (+1.5 m MLLW, 1700 PDT, April 5, 2021) (Google Earth Pro, 2022) had flooded the boulder covered wave-cut platform (WWW Tide and Current Predictor, 2022).

Table 1. Positions of trapped Beeswax Wreck timbers in the NSC site

| Timber # | UTM-E (m) | UTM-N (m) | Timber # | UTM-E (m) | UTM-N (m) |
|---|---|---|---|---|---|
| 1 | 424005 | 5068142 | 14 | 423947 | 5068139 |
| 4 | 424005 | 5068179 | 15 | 423947 | 5068131 |
| 2 | 424003 | 5068162 | 16 | 423943 | 5068127 |
| 3 | 423999 | 5068165 | 17 | 423932 | 5068133 |
| 5 | 423994 | 5068168 | 23 | 423939 | 5068144 |
| 6 | 423992 | 5068168 | 22 | 423933 | 5068148 |
| 7 | 423962 | 5068151 | 21 | 423933 | 5068125 |
| 8 | 423965 | 5068148 | 25 | 423934 | 5068120 |
| 9 | 423963 | 5068140 | 18 | 423935 | 5068117 |
| 10 | 423964 | 5068139 | 26 | 423957 | 5068130 |
| 11 | 423964 | 5068134 | 27 | 423940 | 5068130 |
| 24 | 423952 | 5068134 | 19 | 423938 | 5068138 |
| 13 | 423951 | 5068134 | 20 | 423937 | 5068139 |
| 12 | 423948 | 5068138 | | | |

Notes: Beeswax Wreck timbers, as numbered (#), are presented in UTM (10N) eastings (E) and northings (N) in meters (m). Selected samples of shipwreck timber wood were identified for species (Vitex parviflora) by the Forest Products Research and Development Institute, Department of Science and Technology, Republic of the Philippines. Comparable wood density (very dense) and/or color, such as 2.5Y 7/6 yellow, were used to identify additional shipwreck timbers in the field.

Table 2. Beeswax Wreck timber radiocarbon ages

| Timber # | Radiocarbon age ±1 σ | Calibrated age ±2 σ | Lab # |
|---|---|---|---|
| 6 | 354±22 | cal AD 1528-1796 | D-AMS 039398 |
| 6 | 443±20 | cal AD 1427-1468 | D-AMS 048008/UGAMS61586 |
| 18 | 380±19 | cal AD 1452-1622 | D-AMS 048006/UGAMS61584 |
| 20 | 459±19 | cal AD 1425-1454 | D-AMS 048007/UGAMS6185 |
| 11 | 330±30 | cal AD 1480-1640 | Beta-650643/BWP2022-F011 |
| 14 | 360±30 | cal AD 1456-1634 | Beta-650644/BWP2022-F014 |
| 15 | 400±30 | cal AD 1437-1625 | Beta-650645/BWP2022-F015 |

Notes: Six representative timbers (n=6) from the NSC site were selected and sampled for radiocarbon AMS dating, including two samples from timber # 6. The locations of timbers that were selected for AMS dating are shown in Figure 6 and Table 1. All the calibrated (2 σ) radiocarbon ages are consistent with shipwreck timbers from the Santo Cristo de Burgos, lost in 1693 (Williams et al., 2017, Williams et al., 2018).

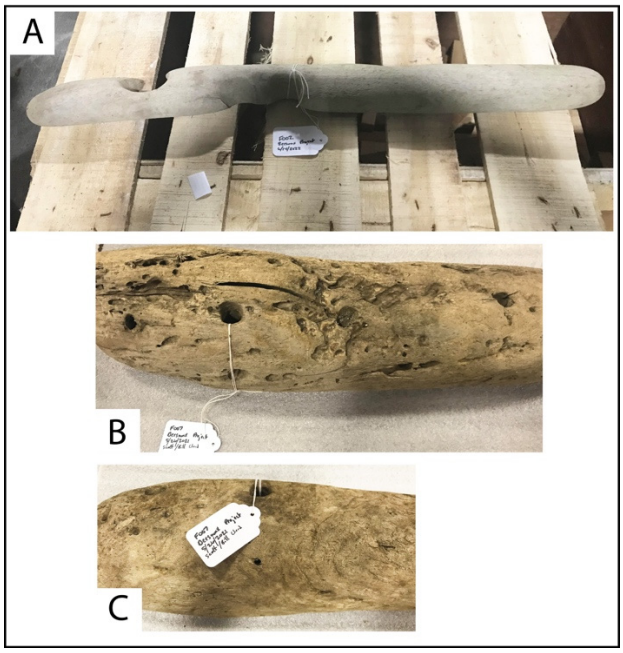


Figure 7. Photographs of two small, buried Beeswax Wreck timbers recovered from the NSC site

Part A, photograph of Beeswax Wreck timber # 2 showing rounding of both ends all four sides by transport abrasion, prior to burial by rockslide boulders. Label (white card) is ~7.5 cm in length. Parts B and C, photographs of opposite sides of one end of Beeswax Wreck timber # 7. The opposite sides show asymmetry of biologic degradation by boring and pitting (degraded side in Part B and undegraded side in Part C), as a function of relative exposure to oxygenated seawater. See Figure 6 and Table 1 for Beeswax Wreck timber positions in the NSC site.

The abundance of entrapped Beeswax Wreck timbers increases greatly with proximity to the west bounding sea cliff projection (Figure 6). Twenty-one entrapped Beeswax Wreck timbers occur in the western side of the site, which is west of Sea Cave 2, whereas only five entrapped Beeswax Wreck timbers were mapped in the vicinity of Sea Cave 1 and only one buried timber was mapped from a position located east of Sea Cave 1. It is not known how many Beeswax Wreck timbers were initially buried by boulders and have since been lost to decay, abrasion, or small boulder movement during extreme wave surge events. It is also unknown whether buried Beeswax Wreck timbers exist in subtidal water depths located offshore the NSC site. The preservation of the 26 buried or pinned Beeswax Wreck timbers on the intertidal wave-cut platform is due to their burial by overlying rockslide debris from one widespread event. There was no observed evidence of multiple layers of buried Beeswax timbers and rockslide debris. Nearly all the observed timbers were found to be in direct contact with underlying bedrock of the wave-cut platform. Modern high resolution satellite images of the north side of Smuggler Cove, taken at low tidal levels during different seasons (Dec. 2011, Jul. 2014, Aug. 2016, and Oct. 2022) (Google Earth Pro, 2022), do not show any accumulations of modern driftwood logs in the NSC site. The very-short residence times of modern driftwood logs in the high-energy wave surge setting of the NSC site, indicate that prior to rockslide burial, the brief accumulation of Beeswax Wreck timbers in the NSC site was anomalous.

In addition to the entrapment of the Beeswax Wreck timbers by overlying large boulders, the initial rockslide debris (see Section 4.5 below) also starved the buried Beeswax Wreck timbers for oxygen, thus preserving the timbers from boring organisms. As the smaller rockslide debris components were selectively removed by wave surge erosion in the NSC site the Beeswax Wreck timbers became increasingly susceptible to boring by marine animals, requiring oxygen. The asymmetry in biogenic degradation on opposite sides of some recovered Beeswax Wreck timbers (Figure 7) demonstrates the burial preservation of Beeswax Wreck timbers from oxidative biologic decomposers over the last several centuries. The timber wood decomposition combined with violent wave surge likely loosened and remobilized some of the buried Beeswax Wreck timber fragments. Some undegraded timbers might underly the thicker boulder ramps located at the foot of the sea cliff just east of Sea Cave 1 (Figure 6), but their more complete burial also hides them from observation. Therefore, the period of buried Beeswax Wreck timber observation is short, being restricted to post-erosion of some rockslide debris but pre-decomposition of the timber artifacts in the intertidal wave-cut platform. The potential preservation of Beeswax Wreck timbers in deeper subtidal water depths, below mean wave surge base, is not known for the NSC site.

*4.2 Mapped Abundances, Distributions, and Sizes of Rockslide Boulders*

Exposed boulders (n~350), of at least 0.5 m intermediate diameter or at least ~0.3 tons in weight, were identified in low-elevation drone images of the narrow intertidal wave-cut platform and overlying boulder ramps (Figures 6 and 8). Several large boulders including boulders I, J, and K, located in front of Sea Cliff 1, were analyzed for surface rounding and relative weathering. Bedding plane and joint fracture surfaces on the large boulder tops showed substantial angularity, indicating little to no rolling or tumbling, of the large boulders by wave surge, after initial rockslide emplacement on the intertidal wave-cut platform. Penetrometer measurements of boulder surfaces and subsurface strata showed >5.0 kg $cm^{-2}$ unconfined shear strength. Twenty of the large rockslide boulders (generally ≥1.0 m intermediate diameter) were selected for size measurement from high resolution drone images (Table 3). Selection of the large boulders was based on their assumed stability after rockslide emplacement and thus representation of rockslide delivery of debris to the wave-cut platform (see Section 4.3 below). Some boulders were also selected based on low tide verification (on site surveys) of Beeswax Wreck timber (burial) association (Figure 6 and Table 3). The representative boulders were georeferenced for position and measured for intermediate diameter in calibrated drone images. Measured boulder sizes ranged from 0.75 to 2.5 m in intermediate axis lengths, as shown in Table 3. Conversion of boulder dimensions to approximate mass, is based on cubed intermediate diameter length multiplied by assumed boulder density of 2.6 t $m^{-3}$. Estimated large boulder masses ranged from 1 to 41 t in the NSC site. Estimated boulder masses decreased from the eastern boulder ramps (5–21 t, boulders A–H) to the westernmost wave-cut platform area, fronting Sea Cave 3 (1–5 t, boulders P–T). The differences in very large boulder (≥1.5 m diameter) and largest boulder (≥2.0 m diameter) abundances appear to reflect different rockslide sources or transport conditions in the separate parts of the NSC site. However, the buried Beeswax Wreck timbers only occur in one stratigraphic horizon, which is immediately above the wave-cut platform bedrock. This is to say that the differences in largest boulder distributions along the length of the NSC site indicate that the rockslide boulders were supplied by multiple, independent, but simultaneous, rockslides in the NSC site (see Section 4.5 below).

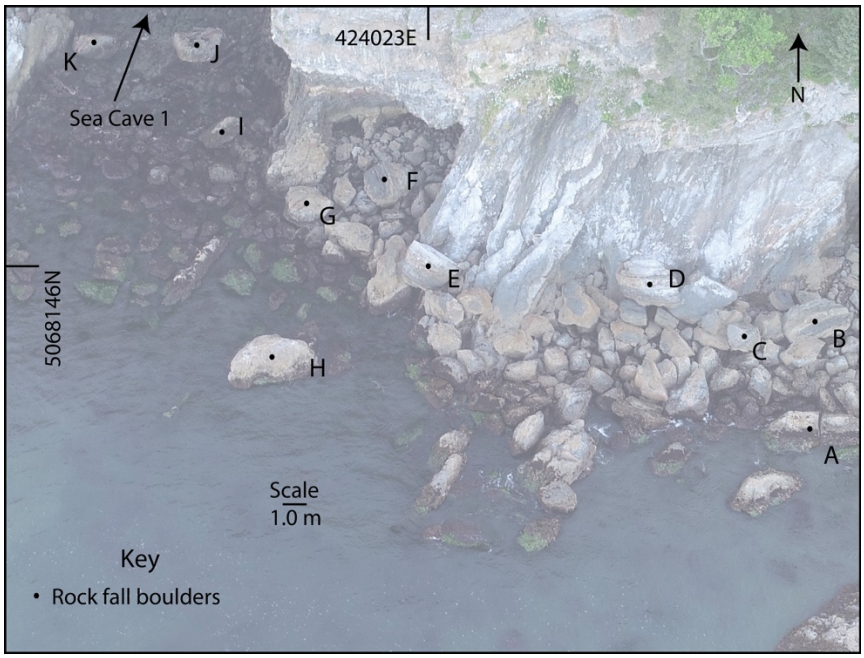


Figure 8. Drone image (June 29, 2018) of rockslide boulders in east side of the NSC site

Mapped features include 1) entrance to Sea Cave 1 and 2) representative large boulders (≥ 1 m in intermediate diameter) lettered A–K from the east side of the NSC site. See Figure 6 for location of Sea Cave 1. Boulder J has buried at least two Beeswax Wreck timbers, and one Beeswax Wreck timber was found wedged under boulder D. Boulder A might have fractured upon impact, as shown by a split along its apparent intermediate axis.

Table 3. Rockslide boulder position, size, and Beeswax Wreck timber association

| Boulder | Easting (m) | Northing (m) | Diameter (m) | Volume ($m^3$) | Mass (t) | Buried timbers |
|---|---|---|---|---|---|---|
| A | 424074 | 5068134 | 2.0 | 8 | 21 | |
| B | 424073 | 5068145 | 1.5 | 3.4 | 9 | |
| C | 424065 | 5068140 | 1.25 | 1.9 | 5 | |
| D | 424058 | 5068143 | 2.0 | 8 | 21 | 1 |
| E | 424039 | 5068140 | 1.5 | 3.4 | 9 | |
| F | 424031 | 5068149 | 1.75 | 5 | 14 | |
| G | 424023 | 5068145 | 1.5 | 3.4 | 9 | |
| H | 424028 | 5068127 | 2.0 | 8 | 21 | |
| I | 424011 | 5068153 | 1.0 | 1 | 3 | |
| J | 424002 | 5068162 | 1.5 | 3.4 | 9 | 2 |
| K | 423993 | 5068161 | 1.0 | 1 | 3 | |
| L | 423985 | 5068161 | 1.5 | 3.4 | 9 | |
| M | 423984 | 5068151 | 1.0 | 1 | 3 | |
| N | 423965 | 5068143 | 2.5 | 15.6 | 41 | 3 |
| O | 423961 | 5068133 | 0.75 | 0.4 | 1 | 1 |
| P | 423949 | 5068132 | 1.25 | 1.9 | 5 | 1 |
| Q | 423947 | 5068126 | 1.25 | 1.9 | 5 | |
| R | 423946 | 5068130 | 1.25 | 1.9 | 5 | 1 |
| S | 423942 | 5068130 | 1.0 | 1 | 3 | 1 |
| T | 423935 | 5068135 | 0.75 | 0.4 | 1 | 1 |

Notes: Boulder position Easting and Northings are in meters (m) UTM-10N. Diameter is intermediate diameter (to the nearest 0.25 m) as measured from calibrated drone images (Figure 8). Volume ($m^3$) is intermediate diameter cubed. Mass in metric tons (t) is calculated from volume ($m^3$) x 2.6 t $m^3$. Buried timbers is the quantity of Beeswax Wreck timber(s) entrapped under the boulder, as mapped on-foot during low tide (Figure 6).

*4.3 Historic Rockslides Used as Analog Models for Sources of NSC Site Boulders*

Two historic rockslides RS1 and RS2, respectively located ~250 and ~150 m east of the NSC site in the north side of Smuggler Cove (Figure 9), are used as analog models for the earlier rockslides that buried the Beeswax Wreck timbers. The RS1 slide occurred in the 1950s in the lower portion of a large hillslope, which reaches >300 m in elevation and >400 m in slope distance from the wave-cut platform (Peterson et al., 2022). A larger prehistoric rockslide (unknown age) apparently delivered boulders to a ridge crest located west (150 m distance) of the RS1 head scarp. The 1950s rockslide (RS1) could have been activated or reactivated by winter storm water discharge from the large hillslope area extending above its head scarp. The 1950s rockslide was about 150 m distance in slope length and 90 m in height (vertical distance). The debris surfaces from the top and middle sections of the rockslide RS1 body are characterized by irregular scarps, hummocks, and angular blocks of sedimentary rock. A smaller historic rockslide RS2 occurred adjacent to the 1950s RS1 rockslide, but the smaller RS2 slide debris was largely revegetated prior to the 1960s aerial photos shown in Figure 9. The smaller historic slide is approximately dated to about 100 years in age, based on the growth diameter of a reoriented spruce tree leader (Figure 10A), assuming a diameter growth rate of ~1 cm $yr^{-1}$ or tree ring growth rate of 0.5 cm $yr^{-1}$ as observed in nearby cut or fallen old growth spruce trees. The smaller rockslide RS2 shows evidence of rockslide debris surface erosion 1) episodic surface water channeling in small rills and 2) by minor downslope movement or creep (Figure 10B). The historically active rills and downslope creep of the rockslide RS2 surface debris serves as analogs for minor surface erosion that might have locally remobilized post-slide debris in the narrow gullies above the NSC site. The

historic RS2 rockslide toe that delivered boulders to the adjacent wave-cut platform has been eroded away by storm surf and/or by surface runoff. In contrast, the younger 1950s rockslide RS1 toe is preserved where it largely covers the buried sea cliff (Figure 9C) The intact rockslide RS1 toe transitions to remanent large boulders on the wave-cut platform. The smaller debris clasts that were delivered to the wave-cut platform by RS1 have been eroded away by storm waves during the last 60–70 years. The intact toe and remnant platform boulders of rockslide RS1 serve as analog models of rockslide boulder distributions that were delivered to the NSC site wave-cut platform. Specifically, the distributions of large boulders (≥1.0 m intermediate diameter) on the rockslide RS1 wave-cut platform are limited to the alongshore extent of the uneroded rockslide toe, as shown in Figure 9C. The largest boulders (≥1.5 m diameter) are restricted to 30–40 m alongshore distance from the center of the rockslide toe. Therefore, the alongshore extent of the largest boulders reflects the locations of the rockslide RS1 toe, body, and head scarp on the steep hillslope above the wave-cut platform.

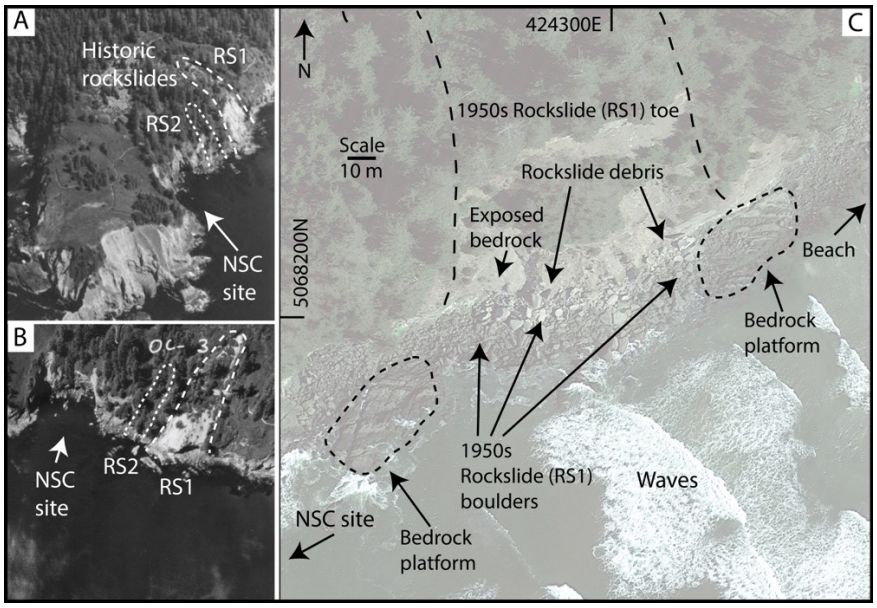


Figure 9. Historic rockslide (RS1 and RS2) and remnant rockslide debris located near the NSC site

Images in Parts A and B are oblique aerial photographs (1960s) of South Cape Falcon showing the relative locations of two historic rockslides RS1 (dashed white line) and RS2 (dotted white line). Photo views in Parts A and B, respectively, are to the east and to the north). Part C, a modern satellite image (2021) shows 1) intact 1950s rockslide RS1 toe (dashed line) and unsorted debris (arrow) above the reach of storm waves, 2) recently exposed sea cliff bedrock (arrow), 3) locally exposed bedrock of the wave-cut platform (dotted line), and 4) large boulders of ≥1.0 m intermediate diameter (arrows) on the wave-cut platform, remaining after 60-70 years of sorting by storm waves.

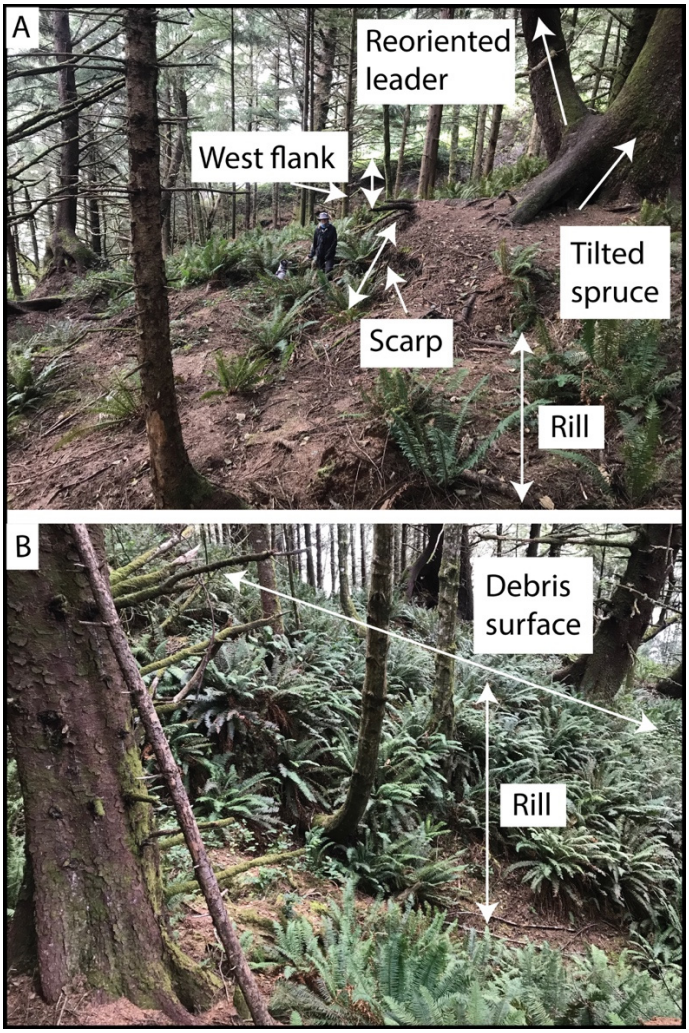


Figure 10. Historic rockslide RS2 mid slope debris surface features

Part A, hummocks, minor scarps, and west slide flank, are shown in historic rockslide RS2 debris, located about 120 m distance east of the NSC site (Figure 9). A slide-tilted, old growth Spruce tree is located above a minor scarp (inclined arrows), about 1.5 m in vertical offset, near the mid-slide area of the rockslide body (see Table 4 in Section 4.5 below). A newer (reorientated) leader of the Spruce tree (~1.0 m in diameter) represents post-slide slope stability. A small rill (~1.0 m depth) in foreground (vertical arrows) demonstrates post-slide erosion from surface water runoff. Photo view is to the west. Part B, mid-slope debris surface (inclined arrows) and small rill (~1.5 m depth) are developed along the west slide flank (~6 m height) of the RS2 rockslide. Some young tree tilting (bent knees) indicates continued minor down slope movement after the earlier major slope failure.

*4.4 Hillslope and Rockslide Geometries of Recent Slope Failures in North Side of Smuggler Cove*

At least six geologically recent rockslides were identified from boulder debris on the wave-cut platform and upslope gullies in the north side of Smuggler Cove (Figures 6 and 11). Two of the rockslides, RS1 and RS2, occurred in historic time (Figures 9 and 10A). One modern or active rockslide site RS7 was investigated on the south side of the Cape Falcon South Point for comparison to the recent past rockslides (Figure 12A). Unlike the historic rockslides, RS1 and RS2, the earlier rockslides above the NSC site, including RS4, RS5 and RS6, have been relatively stable long enough for nearly-vertical-growing spruce trees in the mid slope areas to reach up to ~1.0 m in diameter (Figure 13). Unlike the two historic rockslides, the earlier rockslides above the NSC site did not occur below large hillslopes. Instead, the rockslide RS4, RS5, and RS6 head scarps (70–90 m elevation) above the NSC site occur immediately below the crest of an east-west ridgeline (~100 m elevation) (Figures 9A and 12B). Such short hillslope areas were unlikely to have accumulated sufficient storm rain discharge to have simultaneously activated the multiple, independent rockslides during an extreme rain event. The NSC site rockslides also differ from the modern rockslide RS7, which is located on the south side of the Cape Falcon South Point (Figures 11 and 12A). Whereas the modern rockslide RS7 is directly exposed to southwest wave attack from

winter storms, the sea cliffs in the NSC site are sheltered from direct wave attack by the Cape Falcon South Point and by the small projection of sea cliffs on the west side of the NSC site (Figure 6). The multiple NSC site rockslides that simultaneously buried Beeswax Wreck timbers in the NSC site (see Section 4.2 above) were unlikely to have been activated by an extreme storm wave event. In summary, neither extreme rainfall nor extreme wave energy were likely to have simultaneously triggered the multiple, independent rockslides that buried Beeswax Wreck timbers in the NSC site. As will be discussed later in this article, seismic ground shaking could have served as such a discrete, widespread rockslide-triggering event.

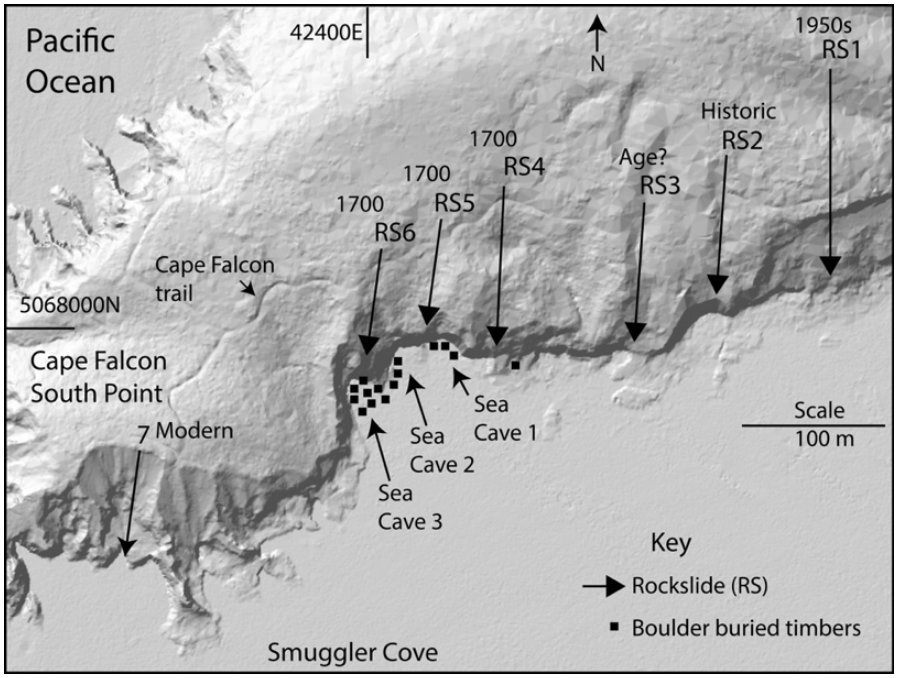


Figure 11. Bare earth lidar hill-shaded DEM image of the NSC site in Cape Falcon

Mapped features include 1) interpreted centers of rockslide courses down shallow gullies in hillslopes above the north side of Smuggler Cove (long arrows) and 2) selected boulder buried Beeswax Wreck timbers on the wave-cut platform (solid squares) in the NSC site. Gullies generally increase in width (downslope), particularly above the cliff tops. Sea Caves 1, 2 and 3 are shown for the NSC site (short arrows). No longitudinal gully features were observed in the RS1 mid-slide area. Lidar hill-shaded digital elevation model (DEM) is from DOGAMI (2022b).

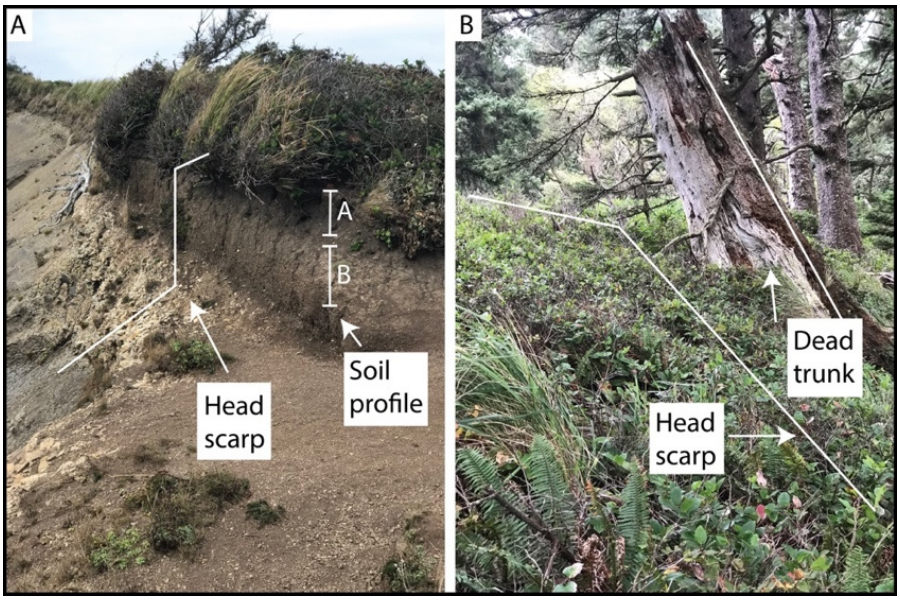


Figure 12. Photographs of head scarps in rockslides from the north side of Smuggler Cove

Part A, the head scarp and laterally adjacent intact soil profile from the slide crown are shown for a modern rockslide RS7 on the south side of Cape Falcon South Point. The well-developed soil profile (organic A horizon ~30 cm thickness and accumulation B horizon ~40 cm thickness) (Table 4) reflects long-term stability of an east-west ridge crest. Photo view is to the west. Part B, photograph shows the vegetation covered head scarp (90 m elevation) of rockslide RS6, located immediately below the ridge crest at ~100 m elevation. The tilted (dead) spruce tree represents head scarp failure, as dated by buried Beeswax Wreck timbers in the front of Sea Cave 3 (Figure 6; Table 2). Vertically growing trees (photo background) post-date the major rockslide. See Figure 11 for rockslide location. Photo view is to the east.

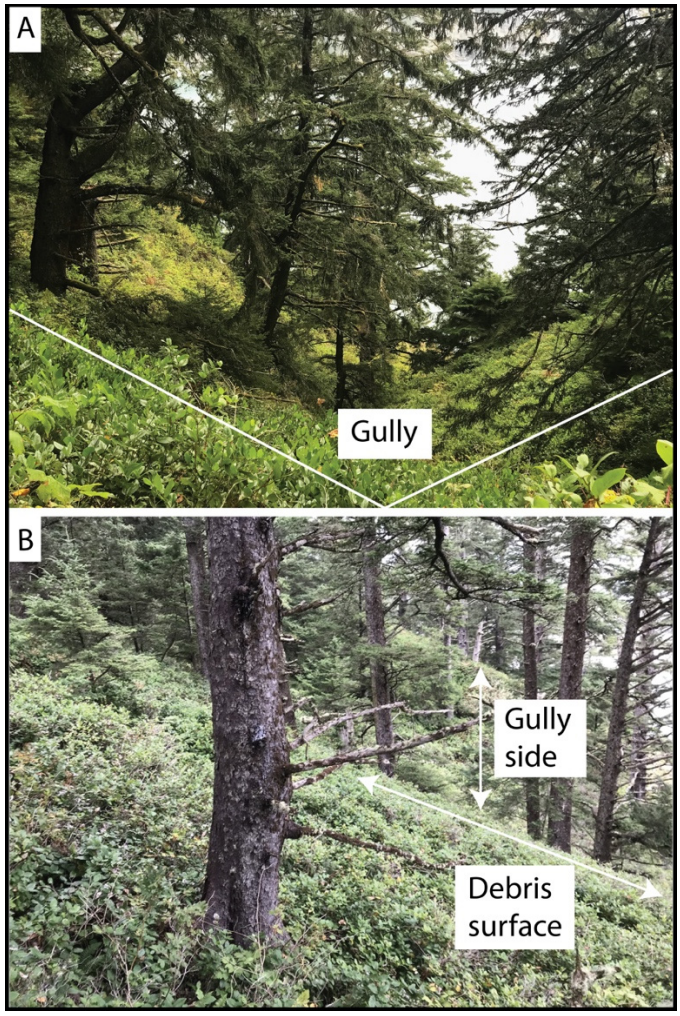


Figure 13. Photographs of rockslide debris and gully in the north side of Smuggler Cove

Part A, a mid-slope gully (~30 m in width and ~7 m in vertical relief) is associated with rockslide RS4 (Table 4). The gully sides were draped with rockslide debris, indicating that the rockslide body reached ≥7 m in thickness. The RS4 gully extends downslope, but it widens above the sea cliff top (Figure 11). Photo is to the south. Part B, mid slope gully in RS6 (Table 4) showing 1) debris surface slope, 2) east gully side or slide flank (~5 m in height), and 3) generally vertical mature tree growth in remnant rockslide debris. Photo view is to the southeast.

*4.5 Thickness and Composition of Remnant Rockslide Debris*

The historic rockslides RS1 and RS2 and the earlier rockslides RS4, RS5, and RS6, which buried the Beeswax Wreck timbers in the NSC site (Figure 11), have been quantitively analyzed for associated gully geometry and rockslide debris components that occur in the gullies (Table 4). Mid-slope gully widths ranged 30–50 m across-slope and demonstrated corresponding vertical relief of 5–8 m as measured between gully bottoms and gully ridge tops. The NSC site rockslides were likely channeled down these gullies, leading to localized rockslide debris toes above the wave-cut platform in the NSC site. Field surveys show that the rockslide debris are characterized by sand/weathered fine gravel, angular pebbles, angular cobbles, and small angular boulders of sedimentary rock (Figure 14; Table 4). The larger angular rock fragments were transported in matrix support

within the rockslide debris bodies. Angular cobbles and small boulders from the mid-slope rockslide debris were fractured by rock hammer, observed for evidence of alteration rims, and measured for minimum shear strengths by calibrated penetrometer. No alteration rims were observed in the rockslide debris cobbles or small boulders. Surface and subsurface rock strengths uniformly exceeded 5.0 kg $cm^{-2}$ unconfined shear strength. The angular cobbles and small boulders in rockslides 1–6 reflect relatively unweathered strata from the Smuggler Cove formation (Cressy, 1974), rather than deeply weathered regolith. The larger debris components were derived from fresh bedrock strata that were fractured during the catastrophic slope failures. No soil B (accumulation) horizons (Birkeland, 1999) are apparent in any of the rockslide debris surfaces. The young geomorphic ages of the rockslide debris are consistent with the expected ages of the historic rockslides and the earlier rockslides in the NSC site. Nearly-vertical growing conifer trees reach 1.0–1.5 m diameter below the head scarps and in mid-slide debris areas of the NSC site rockslides RS4, RS5 and RS6 (Figures 12B and 13). The presence of large, nearly-vertical conifer trees indicates relative slope stability of rockslide areas above the NSC site during the last 100–150 years. These age estimates are based on assumed trunk diameter growth rates of ~1.0 cm $yr^{-1}$, or tree ring growth rates of 0.5 cm $yr^{-1}$, as observed in nearby fallen/cut old growth spruce trees. Furthermore, continuous soil A (organic rich) horizons (10–15 cm thickness) in the soil surfaces of rockslides RS4, RS5 and RS6 (Figure 14D; Table 4) are consistent with relative slope stability since the catastrophic slope failures. That is to say that there is no evidence of major slope failure reactivations of the soil profiles in the NSC site hillslopes since the time of Beeswax Wreck timber burials. Some minor remobilizations of slide debris surface deposits have occurred by surface runoff rilling and by shallow soil creep. Whereas the same post-slide slope stability parameters of the NSC rockslides apply to the undated rockslide RS3 (Figure 11 and Table 4), no buried Beeswax Wreck timbers have been reported for the boulder covered wave-cut platform below the rockslide RS3 gully. The age of the RS3 rockslide is presently not well constrained.

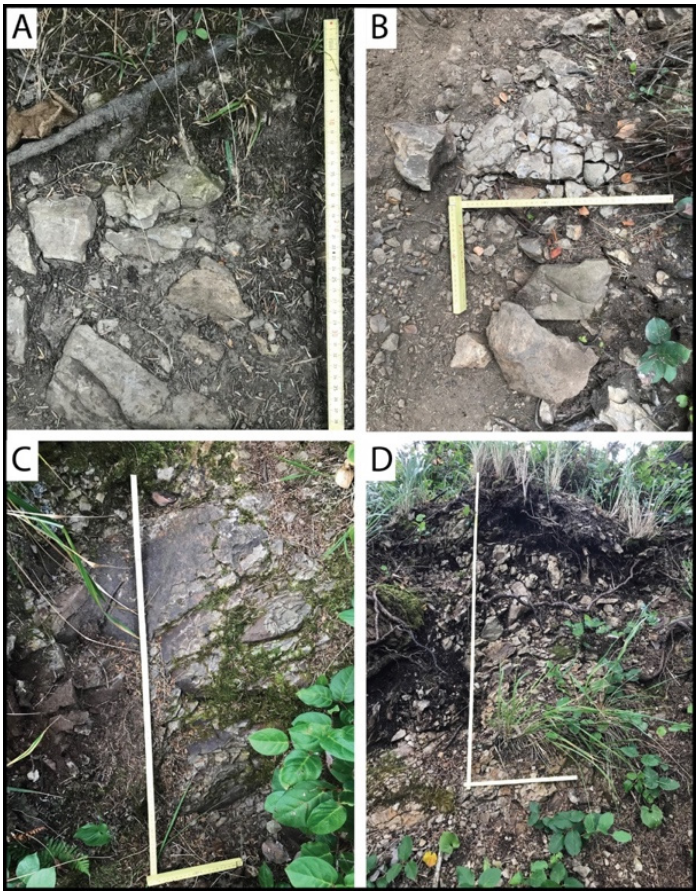


Figure 14. Photographs of rockslide debris and soil horizons as exposed in scarp offsets

Rockslide debris clast sizes are shown in exposed mid-slide scarps from rockslide RS3 (Part A), rockslide RS4 (Part B), rockslide RS5 (Part C), and rockslide RS6 (Part D). Coarse clasts range from angular pebble (0.4–5 cm diameter), to angular cobble (6–25 cm diameter), to angular boulder (>25 cm diameter). Estimates of textural component abundances are shown in Table 4. Shallow soil profiles examined in RS3 (Part A) and RS6 (Part D)

show soil A (organic-rich) horizons to 15 cm depth, but no soil B (accumulation horizons), indicating very-young soil development (Birkeland, 1999). The rockslide locations are shown in Figure 11.

Table 4. Rockslide parameters in the north side of Smuggler Cove

| Site RS (rockslide) # | Head scarp UTM-E (m) | Head scarp UTM-N (m) | Head scarp elevation (m MSL) | Head scarp upslope distance (m) | Upper slide gradient % (degrees°) | Upper slide Soil A / B (cm // cm) |
|---|---|---|---|---|---|---|
| RS1 | 424300 | 5068370 | 80 | 160 | 40 (20°) | 3//0 |
| RS2 | 424210 | 5068280 | 70 | 100 | 50 (25°) | 5//0 |
| RS3 | 424140 | 5068260 | 70 | 100 | 40 (20°) | 15//0 |
| RS4 | 424060 | 5068290 | 70 | 130 | 40 (20°) | 10//10 |
| RS5 | 423990 | 5068250 | 75 | 80 | 40 (20°) | 15//0 |
| RS6 | 423960 | 5068230 | 90 | 80 | 40 (20°) | 15//0 |
| RS7 | 423780 | 5068090 | 65 | 80 | 90 (40°) | 30//40* |
| Site (rockslide) # | Mid-slide gully UTM-E (m) | Mid-slide gully UTM-N (m) | Mid-slide gully width (m) | Mid-slide gully relief (m) | Mid-slide gradient % (degrees°) | Mid-slide composition S/P/C/B (%) |
| RS1 | 424300 | 5068290 | na | na | 60 (30°) | 20/30/40/10 |
| RS2 | 424200 | 5068230 | 40 | 8 | 50 (25°) | 20/50/30/0 |
| RS3 | 424140 | 5068220 | 30 | 5 | 50 (25°) | na |
| RS4 | 424050 | 5068220 | 30 | 7 | 60 (30°) | 10/30/50/10 |
| RS5 | 423990 | 5068210 | 50 | 5 | 50 (25°) | 20/40/30/10 |
| RS6 | 423970 | 5068210 | 30 | 5 | 50 (25°) | 20/20/40/10 |
| RS7 | 423770 | 5068040 | 35 | 10 | 90 (40°) | bedrock |
| Site (rockslide) # | Sea cliff top unvegetated UTM-E (m) | Sea cliff top unvegetated UTM-N (m) | Sea cliff top elevation (m) | Sea cliff top distance (m) | Sea cliff gradient % (degrees°) | Sea cliff strata dip angle (°) S |
| RS1 | na | na | na | na | na | na |
| RS2 | na | na | na | na | na | na |
| RS3 | 424140 | 5068170 | 20 | 30 | 70 (35°) | 30 |
| RS4 | 424060 | 5068180 | 30 | 30 | 100 (45°) | 25 |
| RS5 | 423990 | 5068190 | 50 | 20 | 250 (70°) | 25 |
| RS6 | 423940 | 5068170 | 50 | 30 | 170 (60°) | 25 |
| RS7 | na | na | na | na | na | 25 |

Notes: Head scarp: Rockslide (RS) features include position in meters (m) UTM-10N, approximate elevation (m MSL), approximate upslope distance (m) from the foot of the sea cliff, slope gradient (%) and degree slope angle (°), and thickness (cm) of soil horizon (A) and soil horizon (B) (Birkeland, 1999). Mid-slide debris compositions include relative abundances of sand/fine gravel (S), pebble (P) 0.4-5 cm diameter, cobble (C) 6-25 cm diameter, and boulder (B) >25 cm diameter, as exposed in rockslide debris scarps. Sea cliff tops are taken to be the highest elevations of the unvegetated cliff top. Sedimentary strata dip angles (°) are to the south (S). na=not available.

*4.6 Rockslide Slope Gradients*

Slope gradients of the historic rockslides and the earlier NSC site rockslides RS4, RS5 and RS6, were measured (averaged) over 20–30 m downslope distances, as located in upper rockslides areas below the head scarps and in mid-slide areas located in rockslide gullies (Figure 11). Slope gradients from the upper rockslide debris average 40% (slope angle 20°). The rockslide slopes generally steepen to 50–60% (slope angles of 25–30°) in mid-slide gullies and to ≥100% (slope angle 45°) in the unvegetated sea cliffs in the NSC site (Table 4). The upslope decrease in

slope angles might reflect steeper sea cliff gradients associated with accelerated marine high-stand (Holocene) erosion that is superimposed on pre-existing less-steep gradients developed in the middle and upper slopes during prolonged marine low-stand conditions (late-Pleistocene time). The steep slopes of the active RS7 rockslide (≥90% gradient or 40° slope angle) are the result of rapid sea cliff retreat, resulting from direct wave attack, but not to the much-smaller bedding plane dip angles (~25° dip to the south). Whereas the angles of stability for the modern RS7 rockslide approach 90%, the NSC rockslides failed under the same bedrock conditions in ~50% slopes. The potential mechanism for such low angles of bedrock slope failure in the NSC rockslides are addressed below in Section 5.3. The relatively irregular slopes that descend from the nearly horizontal ridge crest, located above the NSC rockslides, are also apparent in a bare earth lidar slope angle image (Figure 15). However, the very-high resolution of the lidar slope image also represents small scale scarps, hummocks, and rills in the rockslide debris. In addition, the lidar slope image patterns probably reflect some topographic relief from variably resistant bedrock strata beneath the shallowest slide debris cover. The irregularities of the lidar slope image patterns in Figure 15 demonstrate a chaotic small-scale topography superimposed on the generally steep hillslopes in the north side of Smuggler Cove.

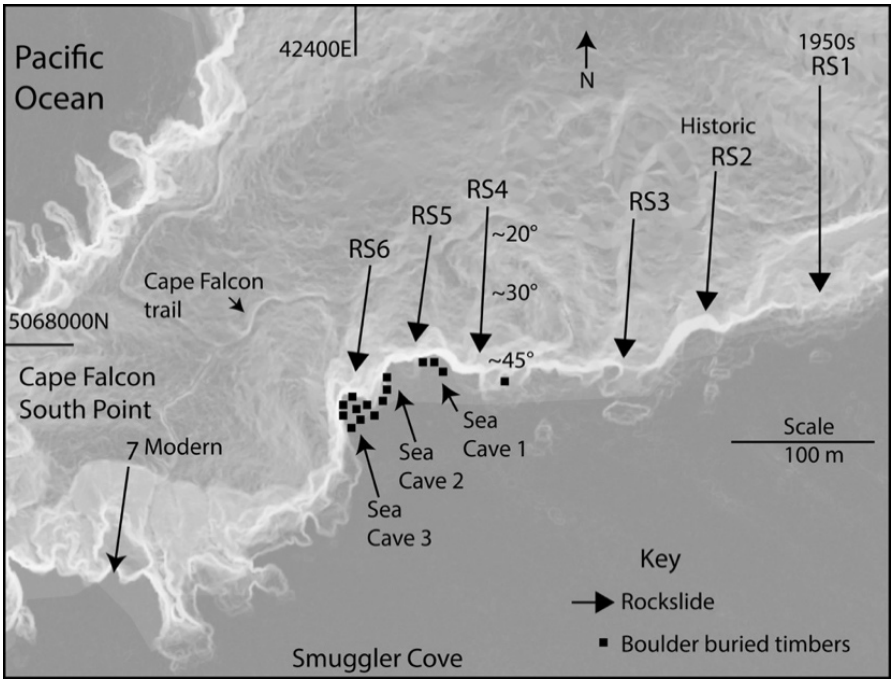


Figure 15. Bare earth lidar slope DEM image of the NSC site in Cape Falcon

Mapped features in the NSC site area include 1) rockslide courses down central gullies (long arrows), 2) spot slope angles (relative brightness), and 3) representative averaged slope angles including, upper slide angle 20° or 40% gradient and mid-slide angle 30° or 60% gradient in RS4 (Table 4). Spot slope angles are locally variable and are generally greater than averaged down-slope angles in the upper and mid-slope areas. The unvegetated sea cliff face in the RS4 gully area is estimated to be 45° or 100% gradient. Sea Caves 1, 2 and 3, and the representative distribution of boulder buried Beeswax Wreck timbers in the NSC site (solid squares) are shown relative to potential hillslope sources of rockslide boulders, as interpreted in Figure 11. Bare earth lidar slope digital elevation model (DEM) is from DOGAMI (2022b).

## 5. Discussion

### *5.1 Storm Wind and Wave Data from Offshore Buoy Records for the Smuggler Cove Study Area*

Major winter storm conditions in the Smuggler Cove study area include strong sustained winds from the south and southwest due to cyclonic flow of storm centers that approach the northern Oregon coast (Byrnes and Li, 1998). To analyze the effectiveness of such winds to transport potential flotsam around the Neahkahnie Mountain headland, wind transport conditions are established based on wind magnitude, direction, duration, and frequency. The rate of driftwood transport or downwind drift is assumed to be 2–4% of free wind velocity, as is well established for wide ranges of driftwood sizes and shapes (Wagner et al., 2022). For example, a due northward blowing wind of 10 m $s^{-1}$ and 5 hours duration could potentially transport Beeswax Wreck timbers from the northernmost early-historic site of tropical wood 'teak' timber recovery in Manzanita to Smuggler Cove, about 5 km in distance (Figure 2).

Northward blowing winds (bearing 180°) are likely to be infrequent, but a wider range of wind directions (bearing 170° to 225°) that include greater durations and frequencies of occurrence could transport Beeswax Wreck wood debris northward, with the assistance of offshore directed rip currents (Figure 16). Offshore directed rip currents from onshore directed storm wave surge at the Neahkahnie Mountain headland are observed to extend ≥0.5 km distance offshore during storm wave conditions. Northward directed geostrophic current flow from storm wind and waves should also help transport driftwood around the Neahkahnie Mountain headland. However, some northward geostrophic flow could also be diverted offshore by downwelling, which leads to seaward directed ocean bottom currents (Kachel and Smith, 1986). Downwelling is not directly relevant to flotsam transport along the ocean surface, so geostrophic flow is neglected here. Higher velocity storm winds (15–20 m $s^{-1}$) and westerly winds (bearing 226-270°), respectively, are neglected in the storm wind compilations due to infrequency and orthogonal incidence with the Neahkahnie Mountain headland.

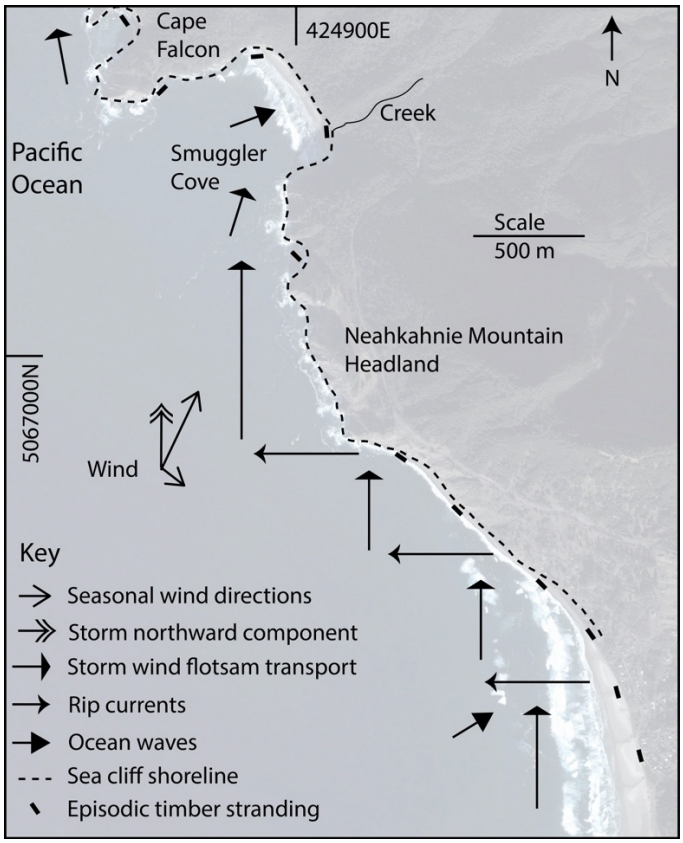


Figure 16. Potential Beeswax Wreck timber transport and stranding during winter storms

Diagramed features include 1) averaged summer and winter storm wind directions (Table 5), 2) the component of northward directed wind transport forcing, 3) observed offshore directed rip currents, 4) storm induced flotsam transport around the Neahkahnie Mountain headland, and 5) episodic Beeswax Wreck timber stranding(s) (bold short lines) in the study area. Base map is from a satellite image taken during winter inter-storm (calm) conditions, December 12, 2005 (Google Earth Pro, 2022). Cloud cover prevents satellite imaging of ocean surfaces during storms.

Modern storm wind and wave data from winter months (December, January, February) are analyzed over a five-year period (2015-2020) from an offshore buoy (46029), located near the mouth of the Columbia River (Figure 1) (NOAA, 2022). The wind data are compiled to help predict whether representative storm wind conditions could have been sufficient in magnitude, direction, duration, and frequency to have transported Beeswax Wreck flotsam debris northward around the Neahkahnie Mountain headland, shortly after the loss of the Santo Cristo de Burgos (Figure 2). Substantial storm wind events are based on velocity magnitude (>10 m $s^{-1}$), direction (bearing 170-225°), and duration (≥ 5 hours). Individual storm wind events of sustained velocity (10–15 m $s^{-1}$) totaled 65 in number for the 2015–2020 winter periods. The sustained durations of the individual storm wind events for all five winter seasons, range 5–47 hour and average 15 hours with a distribution of 15±10 hour 1σ (n=65). Corresponding sustained significant wave heights in deep water ($H_{s\ max1/3}$) range 2–7 m and average 4.0 m, with a distribution of 4.0±1.1 m 1σ (n=65). Corresponding dominant wave period (DWP) is typically 10–14

seconds. A shoaling wave height of 5.2 m is estimated (UCAR, 2022) using 1) a shoaling factor of 1.3 for a DWP of 12 seconds, 2) a $H_s$ of 4.0 m, and 3) a beach steepness of 0.025 over 5–10 m water depths. The wind data are normalized to a northward forcing vector component (11.9 m $s^{-1}$) from mid-range direction (bearing 197°) and mid-range velocity (12.5 m $s^{-1}$). Driftwood transport rate is based on a wind stress transport efficiency of 3% of free wind velocity (Wagner et al., 2022). The driftwood transport rate (m $s^{-1}$) is multiplied by storm wind event duration (hours) to yield the northward driftwood transport distance (km) for each substantial wind event. Individual substantial event distances of potential northward driftwood transport for the five winter seasons range 6–60 km and average 20 km, with a distribution of 20±13 km 1σ (n=65). The monthly totals of computed northward driftwood transport distances are presented in Table 5.

Table 5. Winter monthly totals of computed northward distances of potential driftwood transport

| Year | Month | Wave height ave. $H_s$ (m) | North Wind component (m $s^{-1}$) | Total duration (hours) | Drift distance (km |
|---|---|---|---|---|---|
| 2015 | December | 4.4 | 11.9 | 146 | 188 |
| 2016 | January | 3.8 | 11.9 | 129 | 166 |
| 2016 | February | 4.0 | 11.9 | 74 | 95 |
| 2016 | December | 3.3 | 11.9 | 24 | 31 |
| 2017 | January | 4.0 | 11.9 | 10 | 13 |
| 2017 | December | 3.0 | 11.9 | 28 | 36 |
| 2018 | January | 4.6 | 11.9 | 123 | 159 |
| 2018 | February | 4.0 | 11.9 | 43 | 44 |
| 2018 | December | 4.5 | 11.9 | 60 | 77 |
| 2019 | January | 4.0 | 11.9 | 91 | 117 |
| 2019 | February | 2.7 | 11.9 | 21 | 27 |
| 2019 | December | 4.4 | 11.9 | 49 | 63 |
| 2020 | January | 4.5 | 11.9 | 201 | 259 |
| 2020 | February | 4.0 | 11.9 | 25 | 32 |

Notes: The sustained high-velocity (≥10 m $s^{-1}$) free wind magnitudes for south-southwest wind bearings (170-225°) are taken from NOAA buoy 46029 (Figure 1) records during winter months (Dec, Jan, Feb) for the years 2015–2020. The northward wind component (bearing 180°) of the mid-range wind velocity vector (197° or 17° hypotenuse) is calculated from Cos(hyp angle)*mid-range wind velocity of 12.5 m $s^{-1}$ to yield the velocity of the northward wind forcing component (11.9 m $s^{-1}$). The northward wind drift transport distance is taken from 3% of northward free wind velocity vector multiplied by duration in hours to yield drift distance (km). Net northward estimated potential drift distances are summed and averaged for each month of the winter seasons. Buoy data gaps include February 23-29, 2016, and January 15-February 19, 2017.

On average, 13 potential northward directed events of driftwood transport of at least 20 km distance each occurred per year (winter three-month intervals) for the 2015–2020 period of record. Beeswax Wreck Flotsam transport likely occurred episodically, with multiple stranding and remobilization events from sustained ~5 m breaking wave heights, or shallow water shoaling $H_s$, during the winter seasons. The rounding of most Beeswax Wreck timbers recovered from the NSC site (Section 4.1) attests to abrasion of the timbers in the rocky shorelines during transport and/or during temporary accumulation in the NSC site. The multiple substantial storm-wind events per winter season would likely have been sufficient to transport Beeswax Wreck debris northward along the Nehalem Bay spit and the Neahkahnie Mountain headland to Smuggler Cove (total distances of 7–12 km). Over the periods of several winter seasons the Beeswax Wreck timbers and other shipwreck floating debris would have had more than enough time to reach Smuggler Cove from potential shipwreck sites located offshore of Neahkahnie Mountain headland, the Manzanita beaches, and/or the Nehalem Bay sand spits (Figures 2 and 16). Sustained summer winds, generally 3–8 m $s^{-1}$ in velocity from the northwest (NOAA, 2O22), could have dispersed some Beeswax Wreck flotsam to the south, thus extending the range of stranded Beeswax Wreck wood debris throughout the Beeswax Wreck study area.

*5.2 Predicted Nearshore Currents Leading to Brief Beeswax Wreck Timber Accumulations in the North Side of Smuggler Cove*

Regardless of the Beeswax Wreck location(s), some shipwreck timbers did reach Smuggler Cove (Figure 6). What conditions permitted an accumulation of Beeswax timbers in the NSC site, just prior to rockslide burial? The northwest-southeast orientation of the east end of Smuggler Cove creates an asymmetry in wave nearshore incidence angle, leading to asymmetric longshore currents and increased rip current strength against the south side of Smuggler Cove (Figure 17). The shorter projection of the Neahkahnie headland also promotes greater wave surge against the south side, relative to the north side of Smuggler Cove. Both the reduced wave surge and the relatively weak rip current development along the north side of Smuggler Cove permitted accumulations of Beeswax Wreck timbers in the North Smuggler Cove site, as diagramed in Figure 17. Such localized accumulation of drifting Beeswax Wreck timbers in the North Smuggler Cove site would have been particularly important if the rockslide burial of the timbers occurred during stormy winter months of increased wave height and storm surge (see seasonal timing of rockslide burial of Beeswax Wreck timbers in Section 5.3 below).

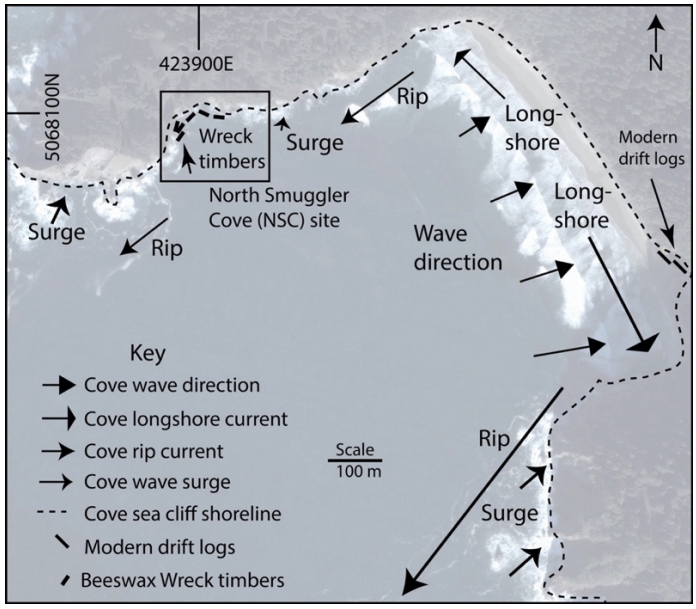


Figure 17. Nearshore currents that lead to localized accumulations of Beeswax Wreck timbers

Diagramed Smuggler Cove nearshore currents derive from 1) cove aligned storm wave directions, 2) slight asymmetry of wave incidence angle and resulting longshore currents that feed seaward directed rip currents, and 3) wave surge in exposed sea cliff shorelines. Beeswax Wreck timbers are expected to briefly accumulate in the NSC site, which is relatively protected from strong rip and wave surge currents. Base map is from a satellite image taken during winter inter-storm (calm) conditions, December 12, 2005 (Google Earth Pro, 2022). Cloud cover prevents satellite imaging of nearshore water surfaces during storms.

The shallow intertidal setting of the wave-cut platform that hosts the buried timbers in the NSC site (Figure 6) limits the size of Beeswax Wreck flotsam that could have been drifted onto the intertidal area. Assuming near equivalence of modern sea level and the sea level at ~300 years ago (Peterson et al., 2020) the upper-intertidal range (1.5 m) and maximum storm surge (~1.5 m) should have limited the size of flotsam (~3 m thickness) that could have floated or washed up onto the upper-intertidal levels of the wave-cut platform. It is not expected that large Beeswax Wreck debris structures could have been emplaced on the intertidal wave-cut platform and/or have survived wave surge pounding against the sea cliffs. Larger shipwreck debris could have been buried in the shallow subtidal water depths located offshore of the NSC site. No surveys for such entrapped Beeswax Wreck debris in the shallow subtidal water depths located offshore of the NSC site (Figure 17) have been performed. An estimated abundance or mass of Beeswax Wreck timbers recovered from the NCS site is estimated to be 200–300 kg dry weight (Section 4.1). A combined weight of 2,500 tons for the galleon (structural wood) and positive-buoyancy bulk cargo (lumber, beeswax, etc.) is assumed for the for Santo Cristo de Burgos (La Follette, 2022). Therefore, the weight of the recovered Beeswax Wreck timbers from the Smuggler Cove (~250 kg or 0.25 tons) represents only 0.01% of potential flotsam from the loss of the Santo Cristo de Burgos. Though Beeswax Wreck structural wood, wood cargo, and beeswax were reportedly recovered from the Nehalem Bay sand spit and Manzanita beach wash-over areas by early European settlers (Williams et al., 2017; Williams et al., 2018) it is not

known how much of the potential Beeswax Wreck flotsam has yet to be recovered or is still located in the study area (Figure 2).

*5.3 Seismic Trigger for Multiple Simultaneous Rockslides that Buried the Accumulated Beeswax Wreck Timbers*

The largest rockslide boulders (≥ 9 t) in the NSC site (Figure 6 and Table 3) are assumed to reflect rockslide routing and boulder emplacement directly below separated gullies in the overlying hillslopes (Figure 11). That is to say that the shore-normal gullies in the NSC site divide delivery routes of the largest boulders into at least three and possibly four rockslide sources or slide areas. Historic rockslides in the study area, including RS1 and RS2 are likely to have been initiated by anomalous high rain fall, as occurs in other sea cliff failure settings in the study region (North, 1964; Priest et al., 2008; Kingen, 2021). The modern rockslide site RS1 is likely reactivated by storm wave erosion removal of slide toe debris. However, these historic rockslides have occurred separately over time. Their initiations are not linked by a single triggering event. Assuming simultaneous burial of the Beeswax Wreck timbers throughout the NSC site, a widespread trigger would have been required to initiate the multiple rockslides in the laterally adjacent hillslope areas. Such a widespread trigger is unlikely to include either extreme rainfall or ocean wave heights because 1) the NSC site rockslide gullies are not developed below large (extended) hillslopes (Figure 11) and 2) the NSC site sea cliffs are not directly exposed to ocean storm waves (Figure 17). The most likely widespread trigger for simultaneous multiple slope failures in the NSC site is strong ground shaking from the coseismic release of elastic strain energy. Such strain energy accumulates in the convergent Central Cascadia Margin between megathrust ruptures, which occur at multi-century recurrence intervals (Darienzo et al., 1990). For example, annual convergent strains measured in the study region of the Central Cascadia Margin range from $10^{-7}$ across some Coast Range profiles to $10^{-8}$ well east of the Cascade volcanic range (Figure 18). Convergent stain rates locally decrease to $10^{-9}$ in north-south trending forearc valleys between the Coast Ranges and the Cascade volcanic arc. Episodic tremor and slip events (ETS) are located under the forearc valleys and the Coast Ranges. The ETS events indicate that some accumulated strain has been released (Cruikshank and Peterson, 2019) but the net accumulated strain over multiple century time scales has been sufficient to have produced great earthquakes, such as the 1700 Cascadia earthquake (~$M_w$ 9.0) in the central Cascadia margin (Cruikshank and Peterson, 2017).

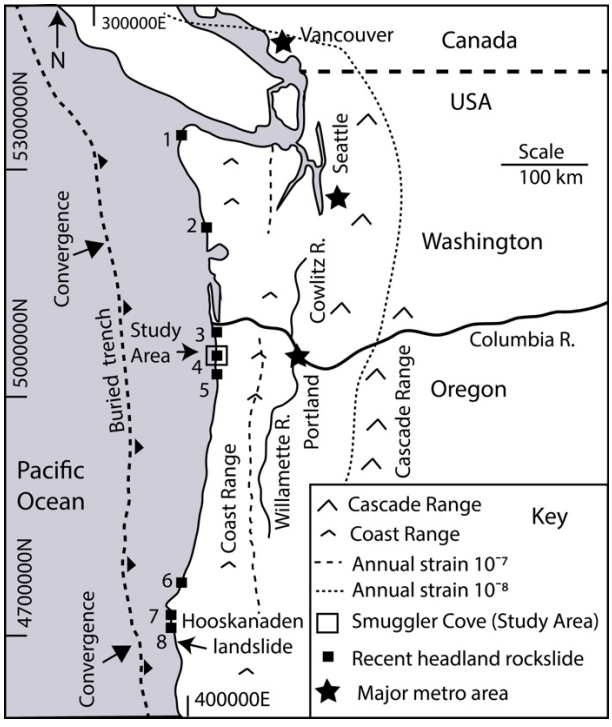


Figure 18. Potential sea cliff rockslide sites that could record seismic shaking from the 1700 Cascadia earthquake

Mapped features include 1) Cascade Range volcanic arc (large pyramids), 2) Coast Ranges (small pyramids), 3) annual strain rates of $10^{-7}$ (dashed line) and $10^{-8}$ (dotted line) (Cruikshank and Peterson, 2019), 4) Smuggler Cove study area (boxed), 5) location of the Hooskanaden landslide complex, 6) major metropolitan areas with populations >500,000 (solid stars), and 7) potential sea cliff/platform sites that might record seismically triggered rockslides (numbered 1–8). The numbered sites include (1) Cape Flattery (53586700N), (2) Cape Elizabeth

(5245000), (3) Tillamook Head (5087200N), (4) Neahkahnie Headland (5066000N), (5) Cape Lookout (5021000N), (6) Cape Arago (4795500N), (7) Port Orford Head (4732800N), and (8) Humbug Mountain (4725300N).

The 1700 Cascadia earthquake has been proposed for the activation or reactivation of the large Hooskanaden landslide complex ($5x10^5$ $m^2$ surface area) in an unstable sea cliff setting in southern Oregon, as shown in Figure 18 (Alberti et al., 2020; Kingen, 2001). However, the Hooskanaden landslide displays 1) ongoing slope failures (interannual slips of ~10 m downslope) that are correlated to high rain fall and 2) ongoing erosion of the landslide toe by ocean storm waves. These ongoing Hooskanaden slope failures complicate the hypothesized mechanisms of coseismic activation and/or reactivation. The small NSC site rockslides (~$3x10^3$ $m^2$ surface area), as shown in Figure 11, do not show evidence of major slope failure after the catastrophic rockslide burial of the Beeswax Wreck timbers (Figure 13). Due to the short residence times of accumulated Beeswax Wreck timbers in the NSC site (Figure 17), the seismic trigger suggested for the NSC site rockslides would have had to occur shortly after the loss of the Santo Cristo de Burgos in 1693 (Williams et al., 2017; Williams et al., 2018). Such a potential seismic trigger did occur from the Cascadia great earthquake in 1700 (Darienzo & Peterson, 1990; Darienzo, et al., 1994; Atwater et al., 1995; Satake et al., 1996), just six years after the loss of the Santo Cristo de Burgos. The several winter seasons of storm winds and waves between the loss of the Santo Cristo de Burgos and the Cascadia earthquake trigger would have been sufficient for the northward transport of Beeswax Wreck timber flotsam around the Neahkahnie Mountain headland and into Smuggler Cove (Table 5; Figure 16). Coincidentally, the seismically triggered rockslides that buried the stranded Beeswax timbers would have occurred well before the arrival of the nearfield tsunami surges that were produced by the 1700 Cascadia megathrust rupture, locally reaching modest runup heights of 7–8 m (Peterson et al., 2015; Minor and Peterson, 2016). Such tsunami inundations in the small Smuggler Cove would have dislodged the Beeswax Wreck timbers from the NSC site had they not been pinned to the wave-cut platform by rockslide debris, just minutes or hours before the nearfield tsunami surges. Sea cliff bounding shorelines throughout Smuggler Cove would have been swept clear of Beeswax Wreck flotsam, unless otherwise buried by rockslide debris just prior to the tsunami inundations. Furthermore, following the tsunami inundations, the entire study area coastline would have experienced ~1.5 m of persistent sea level rise, resulting from coseismic subsidence during the great earthquake (Peterson et al., 2011). During the next ~100 years the wave-cut platform in the NSC site would have remained lower-intertidal -to- subtidal (Cruikshank and Peterson, 2017) therefore, unable to retain any Beeswax Wreck timbers that had not been previously buried and pinned in place by the seismically activated rockslides.

### *5.4 Suggested Additional Sea Cliff Sites for Potential Evidence of Cascadia Earthquake Triggered Rockslides*

The trigger of NSC site rockslides that buried timbers from the Spanish galleon Santo Cristo de Burgos is proposed to have derived from seismic shaking during the 1700 Cascadia earthquake, as discussed in Section 5.3 above. The rockslide burial of Beeswax Wreck timbers in Smuggler Cove, Oregon provides motivation to search for other seismically triggered slope failure sites along the coast of the Central Cascadia Margin (Figure 18). Potential, sea cliff rockslide sites that could record seismic shaking during the 1700 Cascadia great earthquake are proposed here, as based on the following criteria: 1) ≥50 m sea cliff height, 2) south facing rocky headland and/or cove shorelines that demonstrate modern driftwood accumulation, and 3) apparent large boulders (≥1.0 m intermediate diameter) that rest on an intertidal wave-cut platform bedrock. These proposed sea cliff failure sites will not have the unique conditions of the buried Beeswax Wreck timbers to date events of the 1700 Cascadia earthquake-triggered rockslides and/or landslides. However, radiocarbon dating and/or tree ring dating (Yamaguchi, et al., 1997; Dziak et al., 2021) of buried driftwood logs that are pinned to underlying wave-cut platforms could help to provide such timing constraints. Establishing widespread evidence of seismically triggered rockslides and/or landslides in sea cliff slopes in the Central Cascadia Margin would help to confirm and expand estimates of strength of ground shaking from the 1700 Cascadia megathrust rupture along the coast, as shown in Figure 18.

## 6. Conclusions

Shipwreck timbers from the Spanish galleon Santo Cristo de Burgos have been found in a small embayment, Smuggler Cove, located in the northern coast of Oregon. The origin(s) of the shipwreck, locally known as the Beeswax Wreck, have been the source of much speculation since early European settlers arrived in the Nehalem Bay area in the mid-1800s. In addition to beeswax blocks, the Beeswax Wreck debris included porcelain sherds, and tropical hardwood that have been collected across the Nehalem Bay sand spit and in adjacent bay tidal flats. The shipwreck debris was carried across the Nehalem Bay spit by nearfield tsunami surges associated with the 1700 Cascadia subduction zone earthquake. Most recently, shipwreck timbers from the Beeswax Wreck have been found buried under rockslide boulders on a narrow wave-cut platform and in sea caves developed in a recessed sea cliff shoreline in the north side of Smuggler Cove. Smuggler Cove is located ~10 km north of the Nehalem Bay

sand spit. In this study the origins of the large boulders that buried the Beeswax Wreck timbers are tied to rockslides from short steep hillslopes that lie directly above the North Smuggler Cove shipwreck timber burial site. The rockslides are found to have occupied several adjacent, but laterally independent, gullies that simultaneously delivered the large boulders and smaller rockslide debris to the wave-cut platform. Short residence times of driftwood in the high wave-energy Smuggler Cove suggest that the simultaneous rockslides that buried the Beeswax Wreck timbers were activated by a widespread trigger, shortly after the loss of the Santo Cristo de Burgos. Due to variable protection from storm rain runoff and ocean wave impacts the multiple, simultaneous slope failures are attributed to a seismic trigger in the Central Cascadia subduction zone, as opposed to anomalous rainfall and/or storm wave attack. Modern storm wind and rip current analogs suggest that the Beeswax Wreck timbers could have been delivered to Smuggler Cove over a period of several years from sites located 1–10 km south of the south-bounding Neahkahnie Mountain headland. The most likely seismic trigger during this brief time interval is the megathrust rupture of Cascadia subduction zone in 1700 (earthquake magnitude $M_w$~9.0) occurring some six years after the loss of the Santo Cristo de Burgos in late 1693. The results of this study directly address a longstanding uncertainty about the relative strength of shaking from the enigmatic 1700 Cascadia earthquake. Though coastal paleoliquefaction features and nearfield tsunami runups are relatively small for this long-rupture event, it did trigger bedrock rockslides. Such slope failures from a future Cascadia megathust rupture could prevent immediate tsunami evacuations, road transport of emergency relief, and operation of critical power and water infrastructure. The proposed activations of hillslope rockslides in Smuggler Cove by the1700 Cascadia great earthquake provide motivation for further investigations of other potential sites of seismically triggered rockslides in the central Cascadia margin.

**Acknowledgements**

Kara Kingen assisted with early identification of rockslide debris (2020) in the North Smuggler Cove (NSC) study area. Dr. James Delgado, SEARCH Inc., assisted with Beeswax Wreck timber recovery from the NSC site. Jeff Smith, archivist, Columbia River Maritime Museum, assisted with radiocarbon sampling of recovered Beeswax Wreck timbers and estimation of recovered timber weights. Carolyn Peterson assisted with rockslide field surveys (2022) in the NSC study area. Kenneth Cruikshank, Portland State University, provided an early review of rockslide characterizations in the Smuggler Cove study area. Don Pettit, Oregon Department of Environmental Quality, utilized a NOAA contaminant dispersal modeling program (GNOME) to confirm northward flotsam transport along the Nehalem Bay spit during winter storms. Gary Andes provided a non-technical editing review of this article. Radiocarbon AMS dating support for the Beeswax Wreck timbers from the NSC site was provided by the Maritime Archaeology Society, Astoria, Oregon.

**References**

Alberti, S., Senogles, A., Kingen, K., Booth, A., Castro, P., DeKoekkoek, J., Glover-Cutter, K., Mohney, C., Olsen, M., & Leshchinsky, B. (2020). The Hooskanaden Landslide: historic and recent surge behavior of an active earthflow on the Oregon Coast. *Landslides, 17*, 2589-2602. https://doi.org/10.1007/s10346-020-01466-8

Astoria Daily Budget. (1894). *"Ancient Wreckage Ashore."* April 21, 1894 (p. 1).

Atwater, B. F., Nelson, A. R., Clague, J. L., Carver, G. A., Yamagouchi, D. K., Bobrowsky, P. T., Bourgeois, J., Darienzo, M. E., Grant, W. C., Hemphill-Haley, E., Kelsey, H. M., Jacoby, G. C., Nishenko, S. P., Peterson, C. D., & Reinhart, M. A. (1995). Summary of coastal geologic evidence for past great earthquakes at the Cascadia Subduction Zone. *Earthquake Sprectra, 11*, 1-18. https://doi.org/10.1193/1.1585800

Birkeland, P. W. (1999). *Soils and Geomorphology*. Oxford University Press, New York.

Byrnes, M., R., & Li, F. (1998). *Regional analysis of sediment transport and dredged material dispersal patters, Columbia River mouth, Washington/Oregon*. Final Report to US Army Corps of Engineers Waterways Experiment Station. Applied Coastal Research and Engineering, Inc. Mashpee, MA. 53 p

Cressy, F. B. (1974). *Stratigraphy and Sedimentation of the Neahkahnie Mountain-Angora Peak Area, Tillamook and Clatsop Counties, Oregon*. M.S. Thesis, Oregon State University, Corvallis, Oregon.

Cruikshank, K. M., & Peterson, C. D. (2017). Late-stage interseismic strain interval, Cascadia subduction zone margin, USA and Canada. *Open Journal of Earthquake Research, 6*, 1-34. https://doi.org/10.4236/ojer.2017.61001

Cruikshank, K. M., & Peterson, C. D. (2019). Cascadia Convergent Zone: An example of primary convergent seismogenic structure. *Open Journal of Earthquake Research, 8*, 132-164. https://doi.org/10.4236/ojer.2019.82009

Darienzo, M.E., & Peterson, C.D. (1990). Episodic tectonic subsidence of late-Holocene salt marsh sequences in Netarts Bay, Oregon, Central Cascadia Margin, USA. *Tectonics, 9*, 1-22. https://doi.org/10.1029/TC009i001p00001

Darienzo, M. E., Peterson, C. D., & Clough, C. (1994). Stratigraphic evidence for great subduction zone earthquakes at four estuaries in Northern Oregon. *Journal of Coastal Research, 10*, 850-876.

DOGAMI. (2022a). *Geologic Map of Oregon. Interactive Geology Map of Oregon*. Department of Geology and Mineral Resources. Published Online: https://gis.dogami.oregon.gov/maps/geologicmap/. Accessed September 16, 2022.

DOGAMI. (2022b). *Lidar Interactive Map.* Department of Geology and Mineral Resources. Retrieved from https://www.oregongeology.org/lidar/. Accessed September 16, 2022.

Dziak, R. P., Black, B. A., Wei, Y., & Merle, S. G. (2021). Assessing local impacts of the 1700 CE Cascadia earthquake and tsunami using tree-ring growth histories: a case study in South Beach, Oregon, USA. *Natural Hazards and Earth System Sciences, 21*, 1971-1982. https://doi.org/10.5194/nhess-21-1971-2021

Fiedorowicz, B. K. (1997). *Geologic evidence of historic and preshistoric tsunami inundation at Seaside, Oregon*. M.S. Thesis, Portland State University, Portland, Oregon.

Google Earth Pro. (2022). *Earth Pro 2022*. https://www.google.com/earth/. Accessed September 14, 2022.

Giesecke, E.W. (2007). *Beeswax, teak, and castaways: Searching for Oregon's lost protohistoric Asian ship*. Manzanita, OR: Nehalem Valley Historical Society.

Kachel, N. B., & Smith, J. D. (1986). Geologic impact of sediment transporting events on the Washington continental shelf. In: Knight, R. J., McLean, J. R. (eds.), *Shelf Sands and Sandstones, Canadian Society of Petroleum Geologists,* Memoir II, p. 145–162.

Kingen, K. (2021). *Climatic Controls on the Kinematics of the Hooskanaden Landslide, Curry County, Oregon*. M.S. Thesis, Portland State University, Portland, Oregon.

La Follette, C. (2022). *The Manila galleon trade and the wreck on the Oregon coast*. Oregon Historical Society. Published online: https://www.oregonencyclopedia.org/articles/manila-galleon-wreck-on-the-oregon-coast/#.Y459Iy1h1R5. Accessed 12_01_2022.

Ma, L., Wells, R. E., Niem, A. R., Niewendorp, C. A., & Madin, I. P. (2009). *Preliminary Digital Geologic Compilation Map of Part of Northwestern Oregon Oregon Department of Geology and Mineral Industries*, Open-file report 09-03. Published online: https://www.oregongeology.org/pubs/ofr/O-09-03.pdf. Accessed September 20, 2022.

Marshall, D. (1984). *Oregon shipwrecks*. Portland, OR: Binford & Mort.

Minor, R., & Peterson, C.D. (2016). Multiple reoccupations after four paleotsunami inundations (0.3-1.3 ka) at a prehistoric site in the Netarts littoral cell, Northern Oregon, USA. *Geoarchaeology, 32*, 248-266. https://doi.org/10.1002/gea.21593

NOAA. (2022). *Buoy 46029 Historical Data Download Years 2015-2020*. National Oceanic and Atmospheric Administration National Buoy Center. Published online: https://www.ndbc.noaa.gov/download_data.php?filename=46029h2015.txt.gz&dir=data/historical/stdmet/. Accessed December 7, 2022.

North, W.B. (1964). *Coastal landslides in northern Oregon*. M.S. Thesis, Oregon State University, Corvallis, Oregon.

Niem, A. R., & Niem, W. A. (1985). *Geologic map of the Astoria Basin, Clatsop and northernmost Tillamook counties*, northwest Oregon, Oil and Gas Investigation Map OGI-14, plate 1, scale 1:100,000: Portland, Oregon, Oregon Department of Geology and Mineral Industries, Map.

Peterson, C.D., Carver, G.A., Clague, J.J., & Cruikshank, K.M. (2015). Maximum-recorded overland run-ups of major nearfield paleotsunamis during the past 3,000 years along the Cascadia margin, USA and Canada. *Natural Hazards, 77*, 2005-2026. https://doi.org/10.1007/s11069-015-1689-7

Peterson, C.D., Doyle, D.L., Rosenfeld, C.L., & Kingen, K.E.P. (2020). Predicted responses of beaches, bays, and inner-shelf sand supplies to potential sea level rise (0.5-1.0 m) in three small littoral subcells in the

high-wave-energy Northern Oregon Coast, USA. *Journal of Geography and Geology, 12*, 1-27. https://doi.org/10.5539/jgg.v12n2p1

Peterson, C. D., Kristensen, K., & Minor, R. (2014). Large-scale fluidization features from late Holocene coseismic paleoliquefaction in the Willamette River forearc valley, central Cascadia subduction zone, Oregon, USA. *Open Journal of Earthquake Research, 3*, 82-99. https://doi.org/10.4236/ojer.2014.32009

Peterson, C. D., & Madin, I. P. (1997). Coseismic paleoliquefaction evidence in the Central Cascadia Margin, USA. *Oregon Geology, 59*, 51-74.

Peterson, C. D., & Scheidegger, K. F. (1983). *Cascadia earthquake marsh subsidence, tsunami sand layers, and clastic dikes from Alsea Bay, Salmon River estuary, and Willapa Bay*. Marine Geology Seminar, College of Oceanography, Oregon State University, Corvallis, Oregon, Fall Seminar Series, October 1983.

Peterson, C. D., Stock, E., Hart, R., Percy, D., Hostetler, S. W., & Knott, J. R. (2009). Holocene coastal dune fields used as indicators of net littoral transport: West Coast, USA. *Geomorphology, 116*, 115-134. https://doi.org/10.1016/j.geomorph.2009.10.013

Peterson, C. D., Williams, S. S., & Andes, C. N. (2022). *Evidence of rockslide(s) burial of Beeswax Galleon Wreck timbers in a sea cliff-platform site*, North Smuggler Cove, Oregon. Final Field Report Submitted to Maritime Archaeological Society, Astoria, Oregon, November 2022.

Peterson, C. D., Williams, S. S., Cruikshank, K. M., & Duprè J. R. (2011). Geoarchaeology of the Nehalem Spit: redistribution of Beeswax Galleon Wreck debris by Cascadia earthquake and paleotsunami (~ AD 1700), Oregon, USA. *Journal of Geoarchaeology, 26*, 219-244. https://doi.org/10.1002/gea.20349

Priest, G. R., Allan, J. C., Niem, A. R., Niem, W. A., & Dickenson, S. E. (2008). *Johnson Creek Landslide research project, Lincoln County, Oregon: Final report to the Oregon Department of Transportation*. Special Paper 40, Oregon Department of Geology and Mineral Industries, 74 p. Published online: https://rosap.ntl.bts.gov/view/dot/21832. PDF FHWA-OR-RD-08-13, Accessed November 11, 2022.

Satake, K., Shimazaki, K., Tsuji, Y., & Ueda, K. (1996). Time and size of giant earthquake in Cascadia inferred from Japanese tsunami records of January 1700. *Nature, 378*, 246-249. https://doi.org/10.1038/379246a0

UCAR. (2022). *Shallow Water Waves*. Comet Marine Wind and Waves Series Program. University Corporation of Atmospheric Research and National Center for Atmospheric Research. Published online: http://stream1.cmatc.cn/pub/comet/CoastalWeather/sww/comet/marine/SWW/print.htm. Accessed Dec. 12, 2022.

Wagner, T. J. W., Eisenman, I., Ceroli, A. M., & Constantinou, N. C. (2022). How winds and ocean currents influence the drift of floating objects. *Journal of Physical Oceanography, 52*, 907-916. https://doi.org/10.1175/JPO-D-20-0275.1

Williams, S. S., Marken, M., & Peterson, C. D. (2017). *Tsunami and salvage: the archaeological landscape of the Beeswax Wreck*, Oregon. In A. Caparaso (ed). Formation Processes of Maritime Archaeological Landscapes, When The Land Meets The Sea, Springer International Publishing, Cham, Switzerland, p 141-161. https://doi.org/10.1007/978-3-319-48787-8_1

Williams, S. S., Peterson, C. D., Marken, M., & Rogers, R. (2018). The Beeswax Wreck. Special Issue Oregon's Manila Galleon. *Oregon Historical Society, 119*, 192-209. https://doi.org/10.1353/ohq.2018.0049

WWW Tide and Current Predictor. (2022). *WWW Tide and Current Predictor*, Biological Sciences, University of South Carolina, Columbia South Carolina. Published online: http://tbone.biol.sc.edu/tide/. Accessed September 15, 2022.

Yamaguchi, D. K., Atwater, B. F., Bunker, D. E., Benson, B. E., & Reid, M. S. (1997). Tree-ring dating the 1700 Cascadia earthquake. *Nature, 389*, 922-923. https://doi.org/10.1038/40048